Referee #1

General Comments:

"This manuscript represents an extensive approach to compare black carbon (BC) fractions of biomass burning from observations all across the northern hemisphere to GEOS-Chem simulations. The authors further conduct four sets of experiments to test uncertainties associated with the modelling of BC biofuel emissions, BC hygroscopicity, BC ageing, and BC size-resolved scavenging. The overall presentation, language, and figures are of high quality. The study is within the scope of ACP and presents novel data. However, the presentation of the numerical data is currently not up to the desired accuracy. Specifically, it is not always clear if presented percentage numbers are absolute or relative, and uncertainty values are mostly missing or not labeled sufficiently. The used methods and assumptions are mostly clear and valid, yet some conclusions appear vague and a little too uncritical. I suggest to revise the manuscript and focus on accuracy and the specific comments given below."

Specific comments:

1. *"Title: Use a more declarative title. A suggestion: Fossil fuel combustion and biomass burning sources of global black carbon from GEOS-Chem for 2007-2013 compared to observations from 2002-2014."*

Response: Revised.

2. *"f_{bb} values: Is there a reason that no error values or standard deviations are given? In Table S1 all presented values include some form of error. I am writing "some form" because it is not clear what the error value in the table means statistically. What is the confidence interval? Also, sometimes it remains unclear if the values refer to atmospheric or deposition values. For example in L11-171. Please be more specific. Are the presented numbers for atmosphere or deposition?"*

Response: Excellent point. We've added standard deviations in the abstract and added a note in table S1. Clarified f_{bb} values.

Page 1

3. *"L12: Be more specific. What do you mean by "comparable contribution"? Give a number or range."*

Response: Revised accordingly.

4. *"L17: Be more specific. What do you mean with "reduction of discrepancies"? Discrepancies between what?"*

Response: Revised.

5. *"L18: Be more specific. Which "discrepancies" do you mean? "*

Response: Revised.

6. *"L23: Explain what the numbers in the brackets mean. What does this range refer to?"*

Response: Revised accordingly.

7. *"L24-25: This sentence is not very clear. What does increase? Is it concentration, ratios, size or something else? Does "the former" refer to fossil fuels? Replace "the former" with a more specific description.*

Response: Clarified.

8. *"L26-27: Is this finding novel? Please put this, your final conclusion of the abstract, in a bigger context."*

Response: Revised accordingly.

9. *"Abstract in general: Please write a sentence that explains your 4 experiments, in brief and put it before "We find" in L17."*

Response: Done.

Page 2

10. *"L14-16: You write: "Fossil fuel combustion often has an anthropogenic origin". When does it not have an anthropogenic origin? Please change this sentence."*

Response: Done.

11. *"The studies you refer to all looked at local emissions only. Besides that, their assumption is basically the conclusion of your study. Can you reflect more on this in the discussion part of your study?"*

Response: Added discussion in Sect. 5.

Page 3

12. *"L5-15: The model description is very very short. The study would benefit from more detail. Explain why you picked this model and why you think that exactly this set-up (i.e. microphysics scheme, particle size resolution, model resolution, and emission inventories) is best suitable to run the four different tests you laid out before.*

Response: We put the description of the standard simulation in this part and the set-up of the four experiments Sect. 4.3, where we discuss the uncertainties associated with model treatment of various atmospheric processes. The reasons for the set-ups are discussed in Sect. 4.3 as well. We decided to leave this structure as it was for a better flow of the discussion of uncertainties. Because some of the uncertainty experiment designs are

based on the results of the standard simulation.

13. *"L5-6: Please give a reference"*

Response: Revised.

14. *"Discuss in your discussion section what it means for your analysis if you compare observations from 2002-2014 to emission inventories from 2007 publications (in reality the emission information is older than that) or 2017 (in case of Asia)."*

Response: Acknowledged the uncertainties associated with the emission inventories used in Sect. 4.3.6.

15. *"Discuss here how you account for potential double counting of open fire emissions, included as agricultural burning in emission inventories and as open fires in GFED data."*

Response: Open fire emissions were accounted for in a separate biomass emissions inventory and were not included in the biofuel emissions. Thus, there is no potential double counting of open fires from the two inventories.

16. *"briefly explain what updates you applied to the wet deposition scheme of Liu et al., 2001."*

Response: Points well taken. Revised accordingly.

17. *"L16-23: This part appears to be results, rather than model description. Please move it."*

Response: We moved this part to the beginning of Sect. 4.

18. *"L17: Explain why you only simulate 2007-2009 for Fig 1S."*

Response: The data are for 2007-2013. Revised.

19. *"L19: What do you mean by "preferably" ? Can you quantify it?"*

Response: Quantified by correlation coefficient.

20. *"L24-25: Please explain what the criteria was for picking the 41 sites. There is more data available for the observational period you picked (2002-2014) (e.g., (Zotter et al., 2014). You even cite at least one study, who's data you have not included in your analysis, despite falling in that time period (Winiger et al., 2017). Also, is it true that there are only data available from the Northern hemisphere? How confident can you be regarding simulations of the Southern hemisphere, if there is no observational data available?"*

Response: Points well taken. We've tried our best to collect carbon isotope measurements published around the globe. We do not select sites. We've added data from Winiger et al. (2017), Zotter et al. (2014) and Bikkina et al. (2019) Table S1 and relavant analysis in the manuscript.

To our knowledge, there are no data available from the Southern Hemisphere to constrain the model results. Our analysis is based only on model results. This might produce some uncertainties. We acknowledge as such in Sect. 4.3.6.

21. *"L24-25: Why are only the atmospheric samples mentioned in Table S1, when you also discuss the (snow) deposition measurements in your study?"*

Response: We only have carbon isotope analysis of BC in snow over the Tibetan Plateau (Li et al., 2016). We've cited the study in the manuscript.

22. *"Please indicate the measurement technique in Table S1, since there can be considerable differences in BC values between different observational methods (i.e. protocols)."*

Response: Done.

23. *"Please indicate what the error values for f_{bb} mean in Table S1."*

Response: Done.

24. *"Please fix the altitude values in Table S1. Some are 0, e.g., The station in Barrow is at 11 meters above sea level."*

Response: Done.

25. *"The reference for Szidat et al., 2004 (in Table S1) is missing in the SI references."*

Response: Added.

26. *"L25-27: "Generally" is not really accurate. It depends largely on the season. There are cities (in Europe and Asia) where considerable (>40%) f_{bb} values are observed in winter (Zotter et al., 2014, Bikkina et al., 2019)"*

Response: Points well taken. Clarified. We also added carbon isotope observations from Zotter et al. (2014) and Bikkina et al. (2019) in Table S1 and relevant analysis.

Page 4

27. *"L9-L13: This seems to be an important point. The difference in the used methods is bigger than the uncertainties you found with your four experiments. Could you extend on this point? Additionally, add information of the used methods to Table S1."*

Response: The uncertainties associated with observations are added to Sect. 4.3.6. Added used methods to Table S1.

28. *"L10: I would be careful with highlighting single methods. Water extraction is also known to have considerable drawbacks (Azeem et al., 2017). A method for EC extraction (and BC measurements in general, actually) that satisfies all needs is currently nonexistent."*

Response: Excellent point. Revised.

29. *"L15: the factor 2 in Fig.1 (a) is not very clear. Some values (including error) go beyond the factor 2. Could you give these numbers in a table in the Supplementary Information (SI) ?"*

Response: Done. See Table S2.

30. *"L16-22: Please rewrite this. Within the context of these 3 sentences you write 3 times that "the low bias of fbb in [region X] is due to underestimation of biofuel combustion" in one form or another."*

Response: Done.

31. *"L18: What do you mean by "current emission inventories"? Can you give references? You use an emission inventory with emissions older than 2007. Is that also a current emission inventory?"*

Response: Revised.

32. *"L20: While there is little doubt that it is a great study, Qi et al., 2017c is hardly a reference for the sentence that precedes it. It is also not very specific what "large" means. Based on AMAP 2015 (see e.g., their Figure 11.1) European contribution to the BC burden in the Arctic is smaller than that of Russia or East and South Asia (and some other regions, based on the used model). Please consider rewriting this."*

Response: Revised.

33. *"L23: Where can we see the "factor of 2"? This is a general issue in the manuscript. These numbers ("factor of [X]") are presented in many places in the narrative but it is hard to follow. Would it be possible to provide a table in the SI?"*

Response: Done.

34. *"L23: Is there a reason you discuss possible reasons for underestimation of f_{bb} in the Arctic, but decide to discuss overestimates of f_{bb} in North America somewhere else, in Section 4.2.1.?"*

Response: the overestimate of f_{bb} in North America is season dependent, so we discuss it in Section 4.2.1, where seasonal variations are discussed.

35. *"L24-25: What makes you so certain that the large variations of fbb values is "due to the coarse horizontal and vertical resolutions."? Why shouldn't this be the case for all your other modelled cites as well? North-America, for example, has quite some orography as well."*

Response: Points well taken. Revised.

36. *"L30: You write that the model captures the spatial and temporal variations of f_{bb} in BC deposition in this region [Himalayan-Tibetan plateau] and that "GEOS-Chem reproduces the average f_{bb} in snow perfectly". How does that fit with the previous*

comment (L24-25)? Could you discuss this here, instead of section 4.2.1? Your analysis should also be more critical towards the model. What makes you think that the model simulates precipitation well, but less so atmospheric concentrations? Especially since many (if not all) other models struggle with orography (this GEOS- Chem run is at 4°x5° resolution and results discussed are in the Himalaya's !) and deposition schemes (e.g. Textor et al., 2006, Tegen et al., 2019)."

Response: Revised.

37. *"L31-L2 page 5: This sentence is good, because it gives the %-values that makes it possible to follow what you mean with "factor 2.3"."*

Response: Revised accordingly.

38. *"f_{bb} values in general: Please give and define uncertainties for your values or justify why you are not doing so."*

Response: Point well taken. Revised accordingly.

Page 5

39. *"L7-9: You are using annual fossil fuel and biofuel emissions. Why would you expect anything else than "seasonal variation is relatively flat"? Or did you apply some sort of seasonality? This is not clear from reading the model description. Where (daily resolved) open fires (from GFED) too weak in seasonality to show a difference? Or do you attribute this to model resolution entirely?"*

Response: Revised. The emissions are clarified in Sect. 3.

40. *"L11: "probably underestimated" is a very vague formulation. Please be more accurate and specific."*

Response: Deleted.

41. *"L12: It is unclear what you mean with "The similar magnitudes". Similar to what? Consequently, you conclusion of summer values (L12-14) " atmospheric f_{bb} is largely determined by local emissions " is incomprehensible and appears speculative."*

Response: Revised.

42. *"L14: please specify "other seasons"."*

Response: Done.

43. *"L14: please specify if you mean model or observational "atmospheric f_{bb} values"."*

Response: Done.

44. *"L9-15: This entire section appears vague and speculative. Please revise it."*

Response: Revised.

45. *"L15-18: Please give references and write that these are observational values."*

Response: Done.

46. *"L24: " along the Mustang valley and Langtang valley. " To me, it is not clear where these valleys are located. Can you show a figure in the SI?"*

Response: Please see Figures 1 and 2 in Li et al. (2016).

47. *"L24-27: Would you expect any such local effects with the model resolution you are using? Is your model fit for purpose (coarse resolution and no annual resolved emissions) to compare seasonality's in such a terrain? Your conclusion (L29-30) seems not well supported, given the previously mentioned model limitations."*

Response: Revised.

48. *"L31: What do you mean with " no statistically significant differences "? Since you reference the figures here, you could write "no big differences". Better even, give a value for the variations: "no big differences (+/- XX %)"."*

Response: Revised accordingly.

49. *"L32: which "four sites" do you mean?"*

Response: Clarified.

Page 6

50. *"L4-5: What kind of solid fuel would be mostly used, i.e. what are the limited effects on f_{bb} in the atmosphere? According to Mouteva et al., 2017, fraction modern (BC) doesn't change much throughout the year."*

Response: Revised.

51. *"L5-7: I don't think this sentence ("which is proved to have limited effects on f_{bb} (Mouteva et al., 2017)") makes much sense. f_{bb} does not vary much throughout the year. Why would one expect different values during strong winter inversions?"*

Response: Deleted.

52. *"L7-9: Which region are you referring to in this sentence? " Modeled f_{bb} in the atmosphere is much higher than the f_{bb} values of local emissions, suggesting a large regional effect on f_{bb} in this region." I assume it is Salt Lake City, but it is not clear. And where do the numbers come from in " The model overestimates f_{bb} in all seasons by a factor of 2–4. ""*

Response: Clarified.

53. *"L9-10: How does "This mismatch of model representation and observations partly explain[s] the large positive bias of f_{bb}."? 'The model overestimates f_{bb}' is not exactly an explanation of why we see this mismatch."*

Response: Revised.

54. *"L11-12: What kind of regional effect do you mean? What if emissions are wrong? This is an oversimplified analysis."*

Response: Revised.

55. *"L13-14: Which part in the "Comparison of f_{bb} in local emissions and in the atmosphere" suggests that "f_{bb} at MCOH is largely affected by long-range transport..."? Figure 2(g) does not even show if there are local emissions or not."*

Response: Revised.

56. *"L14-15: Please rewrite to reflect that both MOCH and SINH have relatively high f_{bb} (~50%), very similar to each other."*

Response: Revised accordingly.

57. *"L16-30: Please state more clearly when you speak of observation or model."*

Response: Revised accordingly.

58. *"L23-26: It is unclear where the numbers here come from. Also, the highest f_{bb} in the Northern hemisphere is found in African countries, according to your Fig. 3."*

Response: Revised.

59. *"L27-30: Two things: 1. It appears that Antarctica has strong seasonal f_{bb} variation in atmosphere and deposition as well. However, it is a bit hard to quantify this from the figure alone. 2. the "large contribution from open fire emissions" can not be seen in Figs S6 and S7, which show f_{bb} alone. We would need to see BC concentrations before we can conclude that high biomass and biofuel emissions are responsible for the seasonality at the poles."*

Response: 1. Revised. 2. Clarified.

60. *"L29-30: Two things: 1. To write that continental/regional (modelled) data is consistent with observations, when you have mostly one site per region (Fig 2) is a bit of a stretch. Please reflect this limitation more accurately or include more data, e.g., with a table in the SI. 2. Technically you do have one site for Europe, but there (Abisko) is a clear f_{bb} seasonality."*

Response: 1. Points well taken. Revised. 2. Abisko locates inside the Arctic circle. We use "south Europe" instead of "Europe" in the manuscript.

61. *"L3-8: I suggest moving this section to the introduction."*

Response: This part explains why we do the uncertainty analysis associated with biofuel emissions. We think it's better to leave this part in sect. 4.3.1.

62. *"L8: Could you give additional information why you chose to doubled biofuel emissions from domestic heating north of 45°N? Why doubling? why domestic heating ? And why N of 45°N? There is, for example, evidence that open biomass burning might also be underestimated in the Arctic (Konovalov et al., 2018)."*

Response: Revised.

63. *"L11-12: Could you reformulate this? It is not clear to me what you mean by "the model discrepancies... are reduced from -XY% to -YZ%""*

Response: Revised.

64. *"L20: What are the base run conditions for % of hydrophilic fresh biomass burning BC?"*

Response: Revised.

65. *"L21-24: It is not clear what the percentages refer to exactly. If you say that the effect of this experiment lowers atmospheric f_{bb} by "up to 11%", do you mean that the absolute f_{bb} value decreases from e.g., 51% to 40% (-11%) or from 51% to ~46% (-11%)? In the second sentence you write that the largest reductions are "-7%". How does 'largest reduction of -7%' stand in relation to 'lowering of up to 11%'? Please revise these sentences and check the rest of the manuscript as well, where such comparisons take place. Again, a table would eliminate such uncertainties."*

Response: Clarified.

66. *"L26: Can you quantify "large precipitation" ?"*

Response: Done.

67. *"L27-28: It is unclear what you are trying to say with this sentence."*

Response: Revised.

68. *"L29: Which region are you referring to?"*

Response: Revised.

Page 8

69. *"L25: What do the values in brackets mean?"*

Response: Clarified.

70. *"L29-30: Explain why you chose these diameters, since they diverge from the numbers you referred to in L20-21."*

Response: The observed diameters are examples from two studies with both size and coating thickness observations (Revised in the manuscript). The sizes in the model are based on various studies.

71. *"L30: " Size resolved coagulation, condensation, nucleation and cloud processing" are implemented in TOMAS? Please specify or give a reference."*

Response: Clarified.

72. *"L31-L1 page 9: That is an interesting find. Can you elaborate more on the reasons that lead to this effect (i.e. the larger decrease of fossil BC)?"*

Response: Revised.

Page 9

73. *"L20: "within 30%" is a bit unclear. Please be more specific."*

Response: Revised.

74. *"L28: increase " by 18–23%" is a bit unclear. Please be more specific. Essentially this is the same issue with my comment on L21-24, page 7 (see above)."*

Response: Revised.

Page 10

75. *"L8-12: This last paragraph is really disconnected from the rest of the text. Your research doesn't look into mixing states (internal vs external) and lensing. Consider changing it to reflect the scope better."*

Response: Revised.

Figure 1

76. *"Please use more descriptive axes, e.g., "modelled atmospheric BC fraction from biomass burning [%]"."*

Response: Done.

77. *"what standard deviation is shown in the figures?"*

Response: Clarified.

78. *"Could you show error bars in (b)?"*

Response: The standard deviations of observed f_{bb} values are publicly unavailable. We leave it as it was.

79. *"consider different colors in (a) like in your previous publications (e.g. Qi et al., 2017)"*

Response: Done.

80. *"consider using different shapes in (b)"*

Response: Done.

Figure 2

81. *"Why do some sites not have emission bars?"*

Response: All sites have emission bars, but some are too small to be visible.

82. *"Please use more descriptive axes"*

Response: Done.

83. *"There is observational data for Barrow summers available now, see Winiger et al., 2019."*

Response: Added.

84. *"Sometimes the standard deviation bars are not visible. Are they missing? Please specify"*

Response: See response to question #81.

85. *"Is the model grid for each site 4° x5°? Please specify"*

Response: Done.

Figure 3

86. *"Justify why large parts of Indonesia are missing in your regional analysis."*

Response: Included Southeast Asia in the analysis.

Figure 4

87. *"Please use more descriptive axes"*

Response: Done.

88. *"include error bars if possible"*

Response: This is the relative change of mean f_{bb} in each region ($r = ([BC]_{Exp.} - [BC]_{Std.})/[BC]_{Std}$). No error bars.

Figure S2

89. *"Why is the data for 2007-2009, unlike the rest of your study?"*

Response: Revised.

<u>Colorscale</u>

90. *"Just a general comment. Consider a gradual color scale for your maps in future work, that doesn't contain rainbow colors. This is friendlier for color blinds and has the co- benefit that b/w prints are better understandable."*

Response: Sure. Thanks for your suggestions.

Technical corrections

"Please consider the following suggestions:"

<u>Page 1</u>

91. *" L12: remove: Specifically"*

Response: Done.

92. *"L17: replace "northern than" with "north of""*

Response: Done.

93. *" L17-19: Redundancy. Remove "in winter" or "in cold season""*

Response: Done.

94. *" L30: Quantify "large" or remove it."*

Response: Removed.

<u>Page 2</u>

95. *"L2: I assume "BC distribution" refers to atmospheric surface concentrations? Do clarify."*

Response: Clarified.

96. *" L5: Remove "In addition""*

Response: Done.

97. *" L7: Remove "Moreover""*

Response: Done.

98. *" L8-9: Remove the last sentence as it is redundant."*

Response: Done.

99. *" L10: replace "separating" with "distinguishing"."*

Response: Done.

100. *" L16: insert "come" between "can" and "from""*

Response: Done.

101. *L22: There appears to be a word missing after "Alpine""*

Response: Revised.

102. *L23: change "compare" to "compared""*

Response: Done.

103. *L24-25: change to: "The assumption behind these studies is, that the major...""*

Response: Done.

104. *L31: replace "following" with "consecutive""*

Response: Done.

105. *L31: remove "so far""*

Response: Done.

106. *L32: insert "in terms" between "sources" and "of global BC""*

Response: Done.

Page 3

107. *L8: change "3 mn" to "3 nm""*

Response: Done.

108. *"L9: What does MERRA2 stand for?"*

Response: Clarified.

109. *"L20: change " NC_Northest" to " NC_Northeast". Northeast is also misspelled twice in Fig S2 (legend inside right figure)."*

Response: Done.

Page 4

110. *" L3-4: Please give a reference"*

Response: Done.

111. *" L4: change "end member" to "end members""*

Response: Done.

112. *"L4-5: Please give a reference"*

Response: Done.

113. *"L8-9: Please give a reference"*

Response: Done.

114. *"L9: change "thermal-optical method" to " thermal-optical methods""*

Response: Done.

115. *"L15: change "GEOS-Chem simulated fbb in the atmosphere agree with observations within a factor of 2" to "GEOS-Chem simulated atmospheric fbb agrees with observations within a factor of 2""*

Response: Done.

116. *"L24: consider using "horizontal lines" instead of "error bars". The lines show a variation and not actual errors or deviations."*

Response: Points well taken. Revised.

Page 5

117. *"L11: change " to site Abisko " to " to the Abisko site ""*

Response: The sentence is deleted.

118. *"L12: give a reference for the Barrow values."*

Response: Those are model results. Clarified in the manuscript.

119. *"L23: "are shown" where?"*

Response: Clarified.

Page 6

120. *"L3: "area sources" sounds a bit odd. Maybe "non-mobile" is better in this context. Or explain what you mean by it, like they do in Mouteva et al., 2017. (page 9851)."*

Response: Revised accordingly.

121. *"L3: specify "solid" as "wood and coal"."*

Response: Revised.

122. *"L10: Please start a new paragraph for Tokyo data."*

Response: Done.

123. *"L16: consider changing to " 4.2.2 Spatial variation of modelled fbb""*

Response: Points well taken. Done.

124. *" L22: change S3 to S4"*

Response: Done.

Page 7

125. *"L9: In the first instance that "Exp." appears, please write what you mean by it."*

Response: Done.

126. *"L10: change " Specifically " to " As a result ""*

Response: Done.

Page 8

127. *"L25: specify k"*

Response: Done.

128. *"L26-27: This sentence is redundant. Consider removing it"*

Response: Done.

Page 10

129. *"change leaded to led"*

Response: Done.

130. *" Healy et al., 2015 appears to be missing as a reference."*

Response: Revised.

Fossil fuel combustion and biomass burning sources of global black carbon from GEOS-Chem and carbon isotope measurements

Ling Qi[1] and Shuxiao Wang[1,2]

[1]State Key Joint Laboratory of Environment Simulation and Pollution Control, School of Environment, Tsinghua University, Beijing 100084, China
[2]State Environmental Protection Key Laboratory of Sources and Control of Air Pollution Complex, Beijing 100084, China

Correspondence to: Shuxiao Wang (shxwang@tsinghua.edu.cn)

Abstract. We identify sources (fossil fuel combustion versus biomass burning) of black carbon (BC) in the atmosphere and in deposition using a global 3D chemical transport model GEOS-Chem. We validate the simulated sources against carbon isotope measurements of BC around the globe and find that the model reproduces mean biomass burning contribution (f_{bb}, %) in various regions within a factor of 2 (except in Europe, where f_{bb} is underestimated by 63%). GEOS-Chem shows that contribution from biomass burning in the Northern Hemisphere (f_{bb}: 35 ± 14%) is much less than that in the Southern Hemisphere (50 ± 11%). The largest atmospheric f_{bb} is in Africa (64 ± 20%). Comparable contributions from biomass burning and fossil fuel combustion are found in South (S.) Asia (53 ± 10%), Southeast (SE.) Asia (53 ± 11%), S. America (47 ± 14%), S. Pacific (47 ± 7%), Australia (53 ± 14%) and the Antarctic (51 ± 2%). f_{bb} is relatively small in East Asia (40 ± 13%), Siberia (35 ± 8%), the Arctic (33 ± 6%), Canada (31 ± 7%), the US (25 ± 4%), and Europe (19 ± 7%). Both observations and model results suggest that atmospheric f_{bb} is higher in summer (59–78%, vary with sub-regions) than in winter (28–32%) in the Arctic, while it is higher in winter (42–58%) and lower in summer (16–42%) over the Himalayan–Tibetan plateau. The seasonal variations of Atmospheric f_{bb} are relatively flat in North America, Europe, and Asia. We conducted four experiments to investigate the uncertainties associated with biofuel emissions, hygroscopicity of BC in fresh emissions, aging rate and size-resolved wet scavenging. We find that double biofuel emissions for domestic heating north of 45°N increases f_{bb} values in Europe in winter by ~30%, reducing the discrepancy between observed and modeled atmospheric f_{bb} from -63% to -54%. The remaining large negative discrepancy between model and observations suggests that the biofuel emissions are probably still underestimated at high latitudes. Increasing fraction of thickly coated hydrophilic BC from 20% to 70% in fresh biomass burning plumes increases the fraction of hydrophilic BC in biomass burning plumes by 0–20% (vary with seasons and regions), and thereby reduces atmospheric f_{bb} by up to 11%. Faster aging (4 hour e-folding time versus 1.15 days of e-folding time) of BC in biomass burning plumes reduces atmospheric f_{bb} by 7% (1– 14%, vary with seasons and regions), with the largest reduction in remote regions, such as the Arctic, the Antarctic and S. Pacific. Using size resolved scavenging accelerates scavenging of BC particles in both fossil fuel and biomass burning plumes, with a faster scavenging of BC in fossil fuel plumes. Thus, atmospheric f_{bb} increases in most regions by 1–14%. Overall, atmospheric f_{bb} is determined by f_{bb} in emissions mainly and by atmospheric processes, such as aging and scavenging, to a less extent. This confirms the

1

assumption that f_{bb} in local emissions determines atmospheric f_{bb} in previous studies, which compared measured atmospheric f_{bb} directly with local f_{bb} in bottom-up emission inventories.

1 Introduction

Black carbon (BC) in the atmosphere and deposited over snow and ice absorbs solar radiation, triggers positive feedbacks and exerts a positive radiative forcing on the global climate (IPCC, 2014). Estimates of BC radiative forcing span a large range (0.2–1 W m^{-2}, Bond et al., 2013; IPCC, 2014). One of the uncertainties lies in the orders of magnitude different predictions of BC vertical profiles around the globe, particularly in remote regions, by chemical transport and climate models (Samset et al., 2013; 2014). To reduce the uncertainty, in addition to the widely used BC concentration observations in the troposphere, at surface and in snow, observation-based source apportionment (fossil fuel versus biomass burning) of BC provides another dimension to constrain model simulations of BC distribution. The optical properties of BC from fossil fuel and biomass burning plumes are distinctively different (Bond et al., 2013), resulting in different radiative forcing from the two sources (Jacobson, 2010). Because of the relative short lifetime compared to greenhouse gases, accurate source apportionment of BC is important for short-term climate change mitigation.

Carbon isotope analysis is effective in distinguishing emissions from fossil fuel combustion (e.g. coal, oil and natural gas) and contemporary biomass burning (expressed as contribution from biomass burning, f_{bb}, %), because fossil emissions are ^{14}C free and biomass emissions have a characteristic ^{14}C/^{12}C ratio that is proportional to atmospheric carbon dioxide at the time of carbon fixation (Reddy et al., 2002). Combining δ^{13}C and Δ^{14}C measurements further differentiate the contribution from coal and liquid fossil fuel combustion (oil, gasoline and diesel, Andersson et al., 2015 and references therein). Fossil fuel combustion has an anthropogenic origin, including industrial use, domestic cooking and heating, and transport (Bond et al., 2007). Contemporary biomass burning can come from both anthropogenic and natural sources. The former includes mainly industrial and domestic burning of biofuels (fuelwood, charcoal, agricultural residues, and dung, Fernandes et al., 2007) and the latter involves open fires of forests, crops, grass, and peatlands (van der Werf et al., 2010). Carbon isotope measurements are widely used for source apportionment of BC in the atmosphere in South Asia (Gustafsson et al., 2009; Budhavant et al., 2015), East Asia (Chen et al., 2013; Andersson et al., 2015; Zhang et al., 2015; Li et al., 2016), Europe (Szidat et al., 2006; 2009; Zhang et al., 2012) and the Arctic (Barrett et al., 2015; Winiger et al., 2015; 2016; 2017), in snow over the Himalayan-Tibetan Plateau (Li et al., 2016) and in an Alpine ice core (Jenk et al., 2006).

Previous studies (Gustafsson et al., 2009; Chen et al., 2013; Li et al., 2016) compared carbon isotope measurements directly to f_{bb} of local bottom-up emission inventories. The assumption behind these studies is that the major controlling factor of f_{bb} in the atmosphere is local emissions. However, BC-containing particles in fossil fuel and biomass burning plumes have distinctively different mixing states and hygroscopicities (Moteki et al., 2007; Schwarz et al., 2008; Shiraiwa et al., 2007; Akagi et al., 2012), which might further affect BC scavenging in the two kinds of plumes and thus f_{bb} in the atmosphere and after deposition. Li et al. (2016) found smaller contribution from fossil fuel in snow than in air, suggesting that biomass

2

burning emissions are easier to deposit compared to fossil fuel combustion emissions. Possible factors affecting f_{bb} in the atmosphere and in deposition are mixing states and hygroscopicities in freshly emitted fossil fuel and biomass burning plumes, the consecutive aging rate and scavenging. However, as far as we are aware, no study has quantified the contribution of different factors to sources in terms of global BC in the atmosphere and in deposition.

In this study, we simulate sources of BC (fossil fuel combustion versus biomass burning) using a global 3D chemical transport model GEOS-Chem. We describe the model and the carbon isotope measurements in Sections 2 and 3, respectively. We evaluate the model simulation of f_{bb} in Section 4.1, analyze the spatial and temporal variations of f_{bb} in Section 4.2, evaluate the uncertainties associated with f_{bb} in BC emissions, BC mixing state and hycroscopicity in fresh emissions, aging rage and size-resolved scavenging in Section 4.3.

2 Model description

GEOS-Chem is a global chemical transport model driven with assimilated meteorological fields from the Goddard Earth Observing System (GEOS) of the NASA Global Modeling and Assimilation Office (Bey et al., 2001). We use GEOS-Chem v11.01 coupled with the TwO Moment Aerosol Section (TOMAS) microphysics scheme (Adams and Seinfeld, 2002). This is a state-of-the-art global model to simulate global distribution of BC (Wang et al., 2011; Qi et al., 2017 (a and c)). We use 15 size bins ranging from 3 nm to 10 μm with tracers for sulphate, sea salt, organic aerosols, BC, and dust (Pierce et al., 2007; Lee et al., 2009; D'Andrea et al., 2013; Kodros and Peirce, 2017). Modern-Era Retrospective analysis for Research and Applications, Version 2 (MERRA2) meterological data set are used to drive model simulation at 4° latitude × 5° longitude horizontal resolution and 47 vertical layers from the surface to 0.01 hPa. Global fossil fuel and biofuel combustion emissions of BC are from Bond et al. (2007) and Fernandes et al. (2007), respectively. We also include gas flaring emissions from Stohl et al. (2013). We replace BC emissions in Asia by Li et al. (2017). We apply seasonal variations for domestic heating emissions based on degree-day concept (Stohl et al., 2013; Qi et al., 2017c). We use daily open fire emissions from Global Fire Emissions Database version 4 (GFED4, Giglio et al., 2013) in this study. We assume 20% of the freshly emitted BC aerosols are thickly coated and are hydrophilic (Park et al., 2003). We assume hydrophobic BC is converted to hydrophilic with an e-folding time of 1.15 days (Park et al., 2005). Wet deposition follows Liu et al. (2001), with updates of below cloud scavenging efficiency and in-cloud scavenging in ice clouds in Wang et al. (2011) and updates of BC scavenging in mix-phase clouds in Qi et al. (2017a).

3 Observation data

Carbon isotope analysis of BC sources in the atmosphere is available at 65 sites across the globe in different seasons to our knowledge (Table S1 and Fig. S3). Generally, f_{bb} values are larger in remote regions (36±16% in South Asia, 33±14% in the Arctic and 39±17% over the Himalayan–Tibetan plateau) than those in urban regions (13±4% in North America), indicating

a larger contribution from biofuel and open fires in rural, developing and remote regions. In addition, f_{bb} values strongly depend on seasons (see detailed analysis in Sect. 4.2.1). Carbon isotope measurements of BC in snow are only available over the Tibetan Plateau from Li et al. (2016).

Isotope mass balance equation based on the $\Delta^{14}C$ ($^{14}C/^{12}C$) data was applied to apportion the relative contributions to atmospheric BC from biomass burning of modern carbon (f_{bb}) and fossil fuel combustion.

$$\Delta^{14}C = \Delta^{14}C_{bb} f_{bb} + \Delta^{14}C_{ff} (1 - f_{bb}) \qquad (1)$$

Where $\Delta^{14}C$ is the measured radiocarbon content of the BC component and $\Delta^{14}C_{ff}$ is -1,000‰ by definition because fossil carbon is completely depleted in radiocarbon (Li et al., 2016). $\Delta^{14}C_{bb}$ end members used in this equation are usually between +70‰ and +225‰, depending on the type and age of the burned biomass (Winiger et al., 2015; Barrett et al., 2015; Li et al, 2016). The former value corresponds to freshly produced biomass, such as crop and grass. The latter value reflects the burn of wood, which has accumulated over the decades-to-century-long life span. Different choice of the $\Delta^{14}C_{bb}$ end member is one of the uncertainties associated with this source apportionment method. Uncertainty of ±25‰ translates to < 5% in the resulting f_{bb} estimate (Winiger et al., 2016). Another uncertainty stems from the method of isolating BC from total carbon in sampled particles (Zhang et al., 2012). They found that the isolation method prior to thermal treatments, thermal-optical methods, and the heating protocols are important to the isolation of BC and organic carbon and the following isotope analysis. They found that different protocols of thermal-optical method lead to ~ 30% difference of estimated f_{bb} values.

4 Results and Discussions

GEOS-Chem captures the probability density function (PDF) of annual BC concentrations at sites in the US, Europe, China and the Arctic (see site description in Qi et al., 2017(b)) but overestimates the frequency of low BC concentrations (Fig. 1S (a)). About 30% of the simulated annual BC concentration in air is underestimated by a factor of 2 (Fig. 1S (b)). The model reproduces the PDF of BC concentration in snow preferably (correlation coefficient r = 0.98, Fig. 2S (a)). The simulated median BC concentrations in snow in various regions agree with observations within a factor of 2, except in region NC_Northeast Border (Fig. 2S (b)), where the model overestimates the observed BC concentration in snow by a factor of 3 due to the overestimate of local emissions in that region (Qi et al., 2017b).

4.1 Contribution of biomass burning to BC in various regions

GEOS-Chem simulated mean atmospheric f_{bb} in each region agrees with observations within a factor of 2, except in Europe, where f_{bb} is underestimated by 63% (Fig.1 (a)). The low bias of f_{bb} in Europe occurs in non-summer seasons (observation: 45%, model: 13%), which is partly due to the underestimate of biofuel combustion for domestic heating by Fernandes et al. (2007) in most of the European regions during cold seasons (Herich et al., 2011). In South (S.) Asia, mean atmospheric f_{bb} is

4

overestimated by 50%, mostly from the 90% overestimate of f_{bb} at Delhi (observation: 28%, model: 52%). At this site, atmospheric f_{bb} in spring and summer are overestimated by 100% and 200%, respectively. In North America, the model overestimates f_{bb} at Salt Lake City (SLC) and Mexican City by a factor of 2. Possible reasons for the overestimate are explained in Sect. 4.2.1. In the Arctic and East (E.) Asia, the model reproduces the observed f_{bb} values within 3% and 7%, respectively. In addition, GEOS-Chem underestimates the large variations of f_{bb} values (horizontal lines in Fig. 1 (a)) in every region (except in the Arctic), due to the coarse horizontal and vertical resolutions.

Over the Himalayan–Tibetan plateau, observations show that biomass burning dominates BC deposited in snow (64%), but its contribution in the atmosphere is much less (39%, Li et al., 2016). GEOS-Chem reproduces the average f_{bb} in snow (model: 63%) but overpredicts the average atmospheric f_{bb} (model: 62%) by 56%. GEOS-Chem simulated f_{bb} values of BC deposition in snow at all sites over the Himalayan–Tibetan plateau agree with observations within 40% during both monsoon (June–August) and non-monsoon seasons (Fig. 1 (b)), suggesting that the model captures the spatial and temporal variations of f_{bb} in BC deposition in this region. The overestimate of the atmospheric f_{bb} is mainly from 130% overestimate of f_{bb} during monsoon season (observation: 29%, model: 67%). Possible reasons for the overestimate are discussed in Sect. 4.2.1.

4.2 Temporal and spatial variations of f_{bb} in different regions

4.2.1 Temporal variation of f_{bb}

In the Arctic at Abisko, observed f_{bb} ranges from fall and wintertime low of 31% to summer high of 59% (Fig. 2(a)), due to the large contribution from open fires in Europe in summer (Winiger et al., 2016). The model also shows a peak of f_{bb} in summer, but the seasonal variation is relatively flat (from 23% in winter to 27% in summer). We attribute the discrepancy to two reasons. First, f_{bb} values of emissions at the site lack seasonal variations, as shown in Fig.2(a). Second, the coarse resolution does not solve the vortex structure of the low-pressure and frontal systems, which is important for poleward transport of BC (Ma et al., 2014; Sato et al., 2016). At Barrow (Fig. 2 (b)), observed f_{bb} show two peaks in summer (34%) and winter (37%), while modeled f_{bb} shows a single strong peak in summer (78%). In summer, the magnitude and variations of f_{bb} in the atmosphere is similar to that of f_{bb} in local emissions, suggesting that the atmospheric f_{bb} is largely determined by local emissions. The 129% overestimate of f_{bb} is largely due to the overestimate of local open burning emissions. In spring, fall and winter, the modeled atmospheric f_{bb} values are much larger than the f_{bb} of local emissions, indicating a large contribution from long-range transport.

In contrast to the seasonal cycles of f_{bb} at sites in the Arctic, at Bode (Fig. 2(c)) over the Himalayan–Tibetan Plateau, f_{bb} values are the lowest in summer (observation: 17%) and highest in winter (observation: 42%, Li et al., 2016). Similar trend is observed at Lumbini (Fig. 2(d)), only with smaller amplitude (summer low: 42%, spring high: 58%, Li et al., 2016). The lower f_{bb} in summer is because of several reasons. First, less biofuel is consumed for domestic heating in warmer seasons (Li et al., 2016). Second, the region is barely affected by open fires. Third, biomass-sourced BC is removed more efficiently by the frequent precipitation in summer both over the Himalayan–Tibetan plateau and over the surrounding source regions, such

5

as India and East Asia (Li et al., 2016). The GEOS-Chem simulated atmospheric f_{bb} of BC at all sites over the Himalayan–Tibetan plateau (results for Bode and Lumbini are shown in Fig. 2 (c) and (d) and the others are not) have weak or no seasonal variations. In addition, the model does not capture the observed increasing trend of f_{bb} along the Mustang valley and Langtang valley. Possible reasons for the discrepancies are several folds. First, the f_{bb} values of local emissions have no seasonal variations, as shown in Fig. 2 (c) and (d). Second, it is conceivable that the coarse model resolution of global models does not reproduce the complex topography and transport pathways of BC over the Himalayan–Tibetan plateau (He et al., 2014). However, the mean modeled atmospheric f_{bb} generally agrees with observations (within 60%) and the modeled atmospheric f_{bb} generally follows the f_{bb} of local emissions across the whole plateau. These comparisons suggest that the atmospheric f_{bb} over the Himalayan–Tibetan plateau is largely determined by f_{bb} in emissions in the region.

At sites SLC (North America, Fig. 2(e)), Tokyo (East Asia, Fig. 2(f)), MCOH and SINH (South Asia, Fig. 2(g) and (h)), no big differences of f_{bb} among seasons were observed (SLC: 8–13%; Tokyo: 33–41%; MCOH: 52–53%; SINH: 48–56%). However, BC concentrations show strong seasonal variations at the four sites, with high loadings in winter and low loadings in summer (Mouteva et al., 2017; Yamamoto et al., 2007; Budhavant et al., 2015). At SLC, the most significant local sources of $PM_{2.5}$ particles are mobile emissions, which are relatively stable through the whole year (Mouteva et al., 2017). The second most important source is non-mobile sources with solid burning, mostly wood burning, which is not allowed to use when air quality forecasts predict an inversion period (Mouteva et al., 2017). This restriction limits the extra use of solid fuels in winter, and thus limited their effects on BC concentrations and f_{bb} in the atmosphere. So the higher concentration of BC in winter in SLC is largely determined by the low boundary layer height (Mouteva et al., 2017). The model overestimates f_{bb} at SLC in all seasons by a factor of 2–4 (Fig. 2(e)). As described in Mouteva et al. (2017), the observations were in urban environment with strong influence from local emissions. However, modeled f_{bb} in the atmosphere is much higher than the f_{bb} values of local emissions based on emission inventories in this study (Sect. 2), suggesting that the modeled atmospheric f_{bb} at the site is largely affected by the surrounding regions. The misrepresentation of source region (local versus regional) is probably one reason of the large bias of modeled f_{bb} against observations. At site Tokyo, East Asia, the model reproduces both the magnitude and the seasonal variations of observed f_{bb}. The much lower f_{bb} value in emissions than in the atmosphere also indicates a regional effect. In South Asia, GEOS-Chem reproduces the similar observed high f_{bb} values at MOCH (summer: 52%; winter: 53%) and SINH (summer: 48; winter: 56%) within 30%. However, reasons for the high f_{bb} values at the two sites are different. Since there are no local emissions at MCOH, f_{bb} at the site is largely affected by long-range transport. In contrast, f_{bb} in the atmosphere follows f_{bb} in local emissions at SINH, suggesting that the atmospheric f_{bb} at the site is mostly affected by local emissions. At MCOH the high f_{bb} is probably from the large f_{bb} in the outflow of Africa, while at SINH local burning of agricultural crop residues are the major sources (Budhavant et al., 2015).

4.2.2 Spatial variation of modeled f_{bb}

GEOS-Chem suggests that the Southern Hemisphere has a higher contribution from biomass burning both for BC in surface air (50±11%) and in deposition (53±10%, Fig. 3 (a) and (b)). The high f_{bb} in S. America and Australia are largely from active

6

open fires (accounting for 48% and 81% of the total biomass burning contributions, respectively), while in Africa biofuel consumption is the major biomass burning source (model: 64±20%, Fig. 3 (c) and (d)). Because of the strong seasonal variations of open fire emissions, the highest f_{bb} in Africa, S. America, S. Pacific, Australia and the Antarctic usually occur during September to November (58–71%), and the lowest values are in March–May (32–56%, Fig. S4).

In the Northern Hemisphere, the largest f_{bb} of both BC in the atmosphere (93±5%) and in deposition (92±6%) are in North Congo, where biomass burning contribution dominates over fossil fuel emissions. South Asia also shows large f_{bb} (54% for BC in air and in deposition) due to large biofuel consumption. In other regions, such as Europe, Canada, the US, Siberia and the Arctic, fossil fuel contribution (65–80%) is much larger than biomass burning. f_{bb} of BC in air and in deposition in different regions have different seasonal variations (Figs. S4–S5). Atmospheric f_{bb} in Canada, Siberia, the Arctic and the Antarctic have the strongest seasonal variations with a peak in summer (49–70%) because of the large fraction of open fire emissions (Fig. S6–S7). In the US, South Europe, East Asia and South Asia, seasonal variation of f_{bb} is relatively flat, which is also shown by observations at a few sites (Fig. 2).

4.3 Uncertainty analysis

Atmospheric f_{bb} is determined not only by emissions (fossil fuel combustion versus biomass burning), but also by atmospheric processes that affect the deposition during transport. We investigate the uncertainties associated with biofuel emissions, f_{bb} in fresh emissions, BC aging rate and size-resolved scavenging. We used relative change (r, %) to describe the change of f_{bb} in each experiment (Exp.) relative to the standard simulation.

$$r = ([f_{bb}]_{Exp.} - [f_{bb}]_{Std.})/[f_{bb}]_{Std} \qquad (2)$$

where r is the relative change, $[f_{bb}]_{Exp.}$ is f_{bb} in each experiment and $[f_{bb}]_{Std}$ is the f_{bb} in the standard simulation in each region.

4.3.1 Uncertainty associated with biofuel emissions

Biofuel emission estimates are associated with large uncertainties (Fernandes et al., 2007). Source apportionment of BC in Europe based on multi-wavelength aethalometer measurements showed that f_{bb} in winter (24–33%) is much higher than that in summer (2–10%), suggesting that wood burning for domestic heating increases the f_{bb} value in the atmosphere in winter significantly (Herich et al., 2011). In addition, Winiger et al. (2017) analyzed f_{bb} based on carbon isotope measurements at Tiksi in Russia and suggested that domestic (~60% of which is from biomass burning) accounted for 35% of BC at the site, following transport (38%). We find that during cold season mean f_{bb} values in Europe and the Arctic (most sites are north of 45°N, Table S1) are underestimated by 68% and 50% in the standard simulation, probably due to the underestimate of domestic heating in winter. However, in East Asia (all sites are south of 45°N), mean f_{bb} in winter is overestimated by 22%. Thus, we doubled biofuel emissions from domestic heating north of 45°N during cold seasons in Experiment (Exp.) A to

7

investigate the uncertainty associated with biofuel emissions. It is conceivable that the largest effects occur in the Northern four regions, including Europe, Siberia, Canada and the Arctic. As a result, f_{bb} values increase by ~30% in Europe, Siberia and the Arctic and by 15% in Canada in winter, larger than that in spring and fall (4–13%, Fig. 4). Consequently, the low bias of f_{bb} in Europe is reduced from -63% to -54%. This improvement suggests that the biofuel emissions at high latitudes in the Northern Hemisphere are probably too low in current bottom-up BC emission inventories, supporting previous estimates (Herich et al., 2011).

4.3.2 Uncertainty associated with hygroscopicity of BC in freshly emitted biomass burning plumes

Recent measurements find that in freshly emitted fossil fuel plumes the fraction of thickly coated hydrophilic BC is ~10% (Moteki et al., 2007; Schwarz et al., 2008; Shiraiwa et al., 2007), while in biomass burning plumes the fraction reaches up to 70% (Schwarz et al., 2008; Akagi et al., 2012). The higher hygroscopicity of BC in freshly emitted biomass burning plumes enhances the subsequent wet scavenging rate and thereby reduces f_{bb} in the atmosphere. In the standard simulation, we assume 20% of freshly emitted BC particles are hydrophilic. We investigate the effects of the initial hygroscopicity of BC in fresh emissions on atmospheric f_{bb} of BC in Exp. B by assuming 70% of freshly emitted BC particles from biomass burning are thickly coated and hydrophilic. The resulting fraction of hydrophilic BC in biomass burning plumes in the 12 regions increase by 0–20% (vary with seasons and regions), lowering f_{bb} in the atmosphere by up to 11% in Canada in summer. The largest reduction of f_{bb} shows in June–August (-7% averaged for all regions, Fig. 4), when open fires are frequent and active globally (Giglio et al., 2013; van der Werf et al., 2010). During this time, the largest reductions are in Canada (-11%) and Siberia (-10%), where the fraction of hydrophilic BC in biomass burning plumes increases by a large fraction (11–13%). In S. Pacific, the reduction of f_{bb} is large (-10%) as well, because large precipitation (28 kg m^{-2} mon^{-1}) over this region removes more biomass burning BC particles in the outflow of S. America. During September–November, the relative reduction of f_{bb} in the Northern Hemisphere (-6%) is much larger than that in the Southern Hemisphere (-1%), because f_{bb} values in the Southern Hemisphere are too large (Fig. S5). The changes of f_{bb} values in other seasons in all regions are marginal.

4.3.3 Uncertainty associated with BC aging time

Mixing with organic and inorganic particles with larger hygroscopicity, BC particles become more hydrophilic during aging process (Bond et al., 2013). It is assumed that BC particles are converted from hydrophobic to hydrophilic with an e-folding time of 1.15 days after emission in the standard simulation (Park et al., 2005). However, observations showed that the fraction of thickly coated hydrophilic BC in urban fossil fuel plumes increases linearly with plume age (0.5–2.3% h^{-1}, Moteki et al., 2007; Shiraiwa et al., 2007; Subramanian et al., 2010; McMeeking et al., 2011), while BC aging follows a logarithmic trend with an e-folding time of 4 hours in biomass burning plumes (Akagi et al., 2012). The aging rates differ among plumes because of different BC sizes, co-emitted hygroscopic materials and oxidation capacities of the plumes (Bond et al., 2013). Thus, in Exp. C, we assume fossil fuel combustion generated BC ages linearly with a rate of 1% h^{-1}, while BC from biomass burning plumes ages with an e-folding time of 4 hours. This means that the fossil fuel plumes age slower than the standard

simulation and be scavenged slower, while the biomass burning plumes age much faster and are removed from the atmosphere faster in precipitation. This aging scheme leads to a 0–24% increase of fraction of hydrophilic BC in the atmosphere, which reduces f_{bb} by up to -14%. The largest reduction of f_{bb} is in S. Pacific in fall (MAM) and summer (DJF) in the Southern Hemisphere, followed by the Antarctic (-12%) during MAM and the Arctic (-11%) during SON. The reduction of f_{bb} is larger in remote regions and smaller in source regions, because it takes time for the different aging rates in fossil fuel and biomass burning plumes to affect the hygroscopicities of BC in the two plumes and the subsequent aging rates.

4.3.4 Uncertainty associated with size resolved scavenging

BC particles emitted from biomass burning plumes are usually larger in size and thicker in coating thickness (Schwarz et al., 2008; Sahu et al., 2012), suggesting an easier removal from the atmosphere. For example, observations (Schwarz et al., 2008; Sahu et al., 2012) showed that the mass median diameter of BC particles in biomass burning plumes is 193 nm with a coating thickness of 65 nm, while in fossil fuel plumes, the mass median diameter and coating thickness are 175 nm and 20 nm. In addition, because of the different coating materials, hygroscopicities of BC-containing particles in the two kinds of plumes are different as well. The coating materials of BC in urban plumes are dominated by sulfate and followed by nitrate and primary and secondary organics (Shiraiwa et al., 2007), while in biomass burning plumes, the major coating materials are organics (Sahu et al., 2012). For ambient air, characteristic κ values of organics and inorganics are 0.1 (0.01–0.5) and 0.7 (0.5–1.4, Petters and Kreidenweis, 2007; Gunthe et al., 2011 and references therein). Higher hygroscopicity of BC in fossil fuel plumes suggests that they are easier to be activated and serve as CCN compared to BC particles in biomass burning plumes. The higher hygroscopicity and smaller size of BC particles in fossil fuel plumes have opposite effect on their removal rate. Thus, we investigate the total effects of size-resolved scavenging in Exp. D. we use the TOMAS microphysics scheme to process the aging and wet scavenging of BC with different sizes from fossil fuel combustion and biomass burning. The mass median diameters of fossil fuel and biomass burning BC particles are assumed to be 160 nm and 200 nm, respectively. Size resolved coagulation, condensation, nucleation and cloud processing are implemented. Coating materials included are sulfate, nitrate, sea-salt, organics and mineral dust. The size-resolved aging and scavenging scheme leads to a larger increase of fraction of hydrophilic BC in fossil fuel plumes (by 16% (0–31%, vary with regions)) than in biomass burning plumes (by 12% (0–23%)). This increase in both fossil fuel and biomass burning plumes suggest that BC particles are removed faster in the size-resolved simulation than in the standard simulation with a bulk removal parameterization. The larger increase of the fraction of hydrophilic BC in fossil fuel plumes means that BC in fossil fuel plumes are removed faster than those in biomass burning plumes in the size-resolved simulation. This is probably because the total effect of higher hygroscopicity of coating materials and smaller size of BC in fossil fuel plumes is enhancing their removal. Thus atmospheric f_{bb} increases in most regions during MAM (by 1–14%), SON (by 0–7%) and DJF (by 1–12%). The most noticeable characteristics is that the increase of f_{bb} in Northern Hemisphere is larger than those in Southern Hemisphere, due to the large fraction of fossil fuel emissions in the Northern Hemisphere.

9

4.3.5 Uncertainty associated with model resolution

Finer model resolution is capable to reproduce small-scale meteorological conditions, which is critical to BC transport (Sato et al., 2016). We use horizontal resolution of 4° lat × 5° lon in the standard simulation and Exps. A–D, because the size-resolved microphysical scheme TOMAS in Exp. D is computationally expensive. We investigate the uncertainty associated with model resolution in Exp. E by using a finer horizontal resolution of 2° lat × 2.5° lon (Fig. 4). We find that relative to the standard simulation, f_{bb} in Exp. E changes by -5%–5% in the 13 regions in all seasons. In most regions, the absolute change is smaller than or equal to the change in Exp. A–D, except in mid-latitude and tropical regions in Exp. A. Averaged in the whole globe, the relative change of f_{bb} to the standard simulation is -1%.

4.3.6 Other uncertainties

Carbon isotope measurements of BC sources are associated with large uncertainties. Thermal-optical protocol used for the carbon isotope measurements of BC produce ~30% difference of observed f_{bb} values (Zhang et al., 2012), which is equal or larger than the uncertainties of modeled f_{bb} associated with biofuel emissions North of 45°N, aging rate and wet scavenging discussed in Sect. 4.3.1-4.3.4. The comparison of the two sets of data in Sect. 4.1 and 4.2 are within similar uncertainty range. In addition, we do not have carbon isotope measurements in the Southern Hemisphere to constrain the model results. Our analysis in this study is based only on model results.

In addition to the biofuel emissions discussed in Sect 4.3.1, open fire emissions, particularly in the boreal regions, are associated with large uncertainties (Randerson et al., 2012). Konovalov et al. (2018) found that open burning emissions of Siberian fires during May to September from GFED4 is possibly underestimated by a factor of 2 constrained by satellite observations of the aerosol absorption optical depth and the aerosol extinction optical depth. However, we find that during the same season, mean atmospheric f_{bb} at Tiksi in Russia is overestimated by 88%, indicating that open burning emissions in this region from GFED4 are possibly overestimated. This contradiction suggests that further studies are needed to better constrain the open burning emissions in boreal regions. In addition, the global fossil fuel (Bond et al., 2007) and biofuel emission inventory (Fernandes et al., 2007) used in this study are for year 2000 and the emissions in Asia (Li et al., 2017) are for year 2010. We estimated the f_{bb} from 2007 to 2013 using these constant inventories and varying open burning emissions from GFED4. The lack of inter-annual variations of BC fossil fuel and biofuel emissions also produces uncertainties, but it is difficult to quantify based on current knowledge.

5 Conclusions

This study sought to understand the relative contribution of fossil fuel combustion and biomass burning to global BC. We used GEOS-Chem (version 11-01-01) driven by MERRA2 assimilated meteorological fields to simulate BC concentration from fossil fuel and biomass burning. The source apportionment results were expressed as the fraction of BC from biomass

burning (f_{bb}). Simulated f_{bb} was validated against carbon isotope measurements of BC in the atmosphere at 65 stations across the Northern Hemisphere and 11 snow samples over the Himalayan–Tibetan plateau. We also investigated the uncertainties of f_{bb} associated with biofuel emissions, fraction of hydrophilic BC in fresh emissions, aging time and size-resolved scavenging.

5   The model reproduced the mean observed atmospheric f_{bb} in various regions and in snow over the Himalayan–Tibetan plateau within a factor of 2. Generally, values of atmospheric f_{bb} were larger in remote regions (33±14% in the Arctic, 39±17% over the Himalayan–Tibetan plateau and 36±16% in South Asia) than those in urban regions (13±4% in North America), indicating a larger contribution from biofuel and open burning sources in rural, developing and remote regions. f_{bb} was higher in summer (59–78%, vary with regions) than in winter (28–32%, vary with regions)) in the Arctic, while it was

10   higher in winter (42–58%, vary with regions)) and lower in summer (16–42%, vary with regions)) over the Himalayan–Tibetan plateau. The simulated amplitudes of the seasonal variations were much smaller in the two regions. The seasonal variation was observed to be relatively flat in North America, East and South Asia. The simulated monthly mean f_{bb} in these regions agree with observations by -45–275%. The Southern Hemisphere had a higher atmospheric f_{bb} than the Northern Hemisphere (SH: 50±11%, NH: 35±14%) due to the large fraction of open burning emissions in S. America and Australia

15   and large fraction of biofuel consumption in Africa. In the Northern Hemisphere, the highest f_{bb} was in S. Asia (54±10%), followed by E. Asia (41±13%), due to large biofuel consumption. In other regions, such as Europe, Canada, the US, Siberia and the Arctic, f_{bb} values are small (20–35%, vary with regions)).

Simulated f_{bb} was associated with uncertainties from all processes, including emissions, aging and deposition processes. We found that doubled biofuel emissions used for domestic heating north of 45°N resulted in a ~30% increase of f_{bb} in Europe,

20   Siberia and the Arctic and a 15% increase in Canada in winter. This increase reduced the discrepancy of f_{bb} against observations from -63% to -54% in Europe, suggesting that the biofuel emissions at high latitudes were underestimated by the bottom-up emission inventories. Using a higher fraction of hydrophilic BC in fresh biomass burning plumes (uncertainty simulation: 70%, standard simulation: 20%) resulted in a reduction of f_{bb} in summer by -2 – -11%, with the largest reduction in Canada and Siberia, where open fires were frequent. In the standard simulation, it was assumed that BC in both fossil fuel

25   and biomass burning plumes aged following an e-folding time of 1.15 days. In the uncertainty simulation, we used a 4 hour e-folding life time for BC in biomass burning plumes and a linear aging rate of 1% for BC in fossil fuel plumes. This led to a reduction of f_{bb} up to -14% in the atmosphere. The largest reduction was in S. Pacific in fall (MAM) and summer (DJF) in the Southern Hemisphere. The reductions in the Antarctic (-12%) and the Arctic (-11%) were also large in fall when there were large open fires in the Southern Hemisphere and at high latitudes in the Northern Hemisphere. Size-resolved aging and

30   scavenging scheme led to a larger increase of fraction of hydrophilic BC in fossil fuel plumes (by 16% (0–31%)) than in biomass burning plumes (by 12% (0–23%)). Thus atmospheric f_{bb} increased in most regions during MAM (by 1–14%), SON (by 0–7%) and DJF (by 1–12%). Using finer model resolution produced -5%–5% relative change of atmospheric f_{bb} in the various regions, equal or smaller than the change caused by atmospheric processes.

This study showed that local emissions had a larger effect on atmospheric f_{bb} than other atmospheric processes. As discussed in Sect. 1, most previous studies compared measured atmospheric f_{bb} directly with f_{bb} in local emissions. We confirmed this assumption, but suggested considering the uncertainties associated with aging and scavenging (up to 14%). In addition, ~30% difference of isotope-based measurements of f_{bb} caused by the thermal-optical protocols in measuring BC should also be considered.

This study has important implications for estimating radiative forcing of global BC. Previous studies (Healy et al., 2015 and references therein) showed that BC-containing particles in open fires had no optical lensing effect. Considering the large contribution from biomass burning in S. Asia, SE. Asia and in the Southern Hemisphere as suggested in this study, the inclusion of lensing-related absorption enhancement in climate models for BC from both fossil fuel combustion and biomass burning sources may lead to an overestimate of the radiative forcing of global BC. Measurements of the optical properties of BC particles from different sources (fossil fuel versus biomass burning) in different regions are needed to better constrain its radiative forcing.

Author contribution

Ling Qi and Shuxiao Wang designed the experiments. Ling Qi performed the simulations. Ling Qi prepared the manuscript with contributions from Shuxiao Wang.

References

Adams, P. J., and Seinfeld, J. H.: Predicting global aerosol size distributions in general circulation models, Journal of Geophysical Research: Atmospheres, 107(D19), 4370-4392, doi:10.1029/2001JD001010, 2002.

Akagi, S. K., Craven, J. S., Taylor, J. W., McMeeking, G. R., Yokelson, R. J., Burling, I. R., Urbanski, S. P., Wold, C. E., Seinfeld, J. H., Coe, H., Alvarado, M. J., and Weise, D. R.: Evolution of trace gases and particles emitted by a chaparral fire in California, Atmospheric Chemistry and Physics, 12, 1397-1421, doi:10.5194/acp-12-1397-2012, 2012.

Andersson, A., Deng, J., Du, K., Zheng, M., Yan, C., Skold, M., and Gustafsson, O.: Regionally-varying combustion sources of the January 2013 severe haze events over eastern China, Environ Sci Technol, 49, 2038-2043, doi:10.1021/es503855e, 2015.

Barrett, T. E., Robinson, E. M., Usenko, S., and Sheesley, R. J.: Source Contributions to Wintertime Elemental and Organic Carbon in the Western Arctic Based on Radiocarbon and Tracer Apportionment, Environ Sci Technol, 49, 11631-11639, doi:10.1021/acs.est.5b03081, 2015.

Bey, I., D. J. Jacob, R. M. Yantosca, J. A. Logan, B. Field, A. M. Fiore, Q. Li, H. Liu, L. J. Mickley, and M. Schultz, Global modeling of tropospheric chemistry with assimilated meteorology: Model description and evaluation, Journal of Geophysical Research, 106, 23073-23095, https://doi.org/10.1029/2001JD000807, 2001.

Bikkina, S., Andersson, A., Kirillova, E. N., Holmstrand, H., Tiwari, S., Srivastava, A. K., Bisht, D. S., and Gustafsson, Ö.: Air quality in megacity Delhi affected by countryside biomass burning, Nature Sustainability, 2, 200-205, doi:10.1038/s41893-019-0219-0, 2019.

Bond, T. C., Bhardwaj, E., Dong, R., Jogani, R., Jung, S., Roden, C., Streets, D. G., and Trautmann, N. M.: Historical emissions of black and organic carbon aerosol from energy-related combustion, 1850-2000, Global Biogeochemical Cycles, 21, GB2018, doi:10.1029/2006gb002840, 2007.

Bond, T. C., Doherty, S. J., Fahey, D. W., Forster, P. M., Berntsen, T., DeAngelo, B. J., Flanner, M. G., Ghan, S., Kärcher, B., Koch, D., Kinne, S., Kondo, Y., Quinn, P. K., Sarofim, M. C., Schultz, M. G., Schulz, M., Venkataraman, C., Zhang, H., Zhang, S., Bellouin, N., Guttikunda, S. K., Hopke, P. K., Jacobson, M. Z., Kaiser, J. W., Klimont, Z., Lohmann, U., Schwarz, J. P., Shindell, D., Storelvmo, T., Warren, S. G., and Zender, C. S.: Bounding the role of black carbon in the climate system: A scientific assessment, Journal of Geophysical Research: Atmospheres, 118, 5380-5552, doi:10.1002/jgrd.50171, 2013.

Budhavant, K., Andersson, A., Bosch, C., Kruså, M., Kirillova, E. N., Sheesley, R. J., Safai, P. D., Rao, P. S. P., and Gustafsson, Ö.: Radiocarbon-based source apportionment of elemental carbon aerosols at two South Asian receptor observatories over a full annual cycle, Environmental Research Letters, 10, 064004, doi:10.1088/1748-9326/10/6/064004, 2015.

Chen, B., Andersson, A., Lee, M., Kirillova, E. N., Xiao, Q., Krusa, M., Shi, M., Hu, K., Lu, Z., Streets, D. G., Du, K., and Gustafsson, O.: Source forensics of black carbon aerosols from China, Environ Sci Technol, 47, 9102-9108, doi:10.1021/es401599r, 2013.

D'Andrea, S., Häkkinen, S., Westervelt, D., Kuang, C., Levin, E., Kanawade, V., Leaitch, W., Spracklen, D., Riipinen, I., and Pierce, J.: Understanding global secondary organic aerosol amount and size-resolved condensational behavior, Atmospheric Chemistry and Physics, 13(22), 11519-11534, doi: 10.5194/acp-13-11519-2013, 2013.

Fernandes, S. D., Trautmann, N. M., Streets, D. G., Roden, C. A., and Bond, T. C.: Global biofuel use, 1850-2000, Global Biogeochemical Cycles, 21(2), GB2019, doi:10.1029/2006gb002836, 2007.

13

Giglio, L., Randerson, J. T., and van der Werf, G. R.: Analysis of daily, monthly, and annual burned area using the fourth-generation global fire emissions database (GFED4), Journal of Geophysical Research: Biogeosciences, 118(1), 317-328, doi:10.1002/jgrg.20042, 2013.

Gunthe, S. S., Rose, D., Su, H., Garland, R. M., Achtert, P., Nowak, A., Wiedensohler, A., Kuwata, M., Takegawa, N.,

5   Kondo, Y., Hu, M., Shao, M., Zhu, T., Andreae, M. O., and Pöschl, U.: Cloud condensation nuclei (CCN) from fresh and aged air pollution in the megacity region of Beijing, Atmospheric Chemistry and Physics, 11, 11023-11039, doi:10.5194/acp-11-11023-2011, 2011.

Gustafsson, Ö., Kruså, M., Zencak, Z., Sheesley, R. J., Granat, L., Engström, E., Praveen, P., Rao, P., Leck, C., and Rodhe, H.: Brown clouds over South Asia: biomass or fossil fuel combustion?, Science, 323, 495-498, doi:

10   10.1126/science.1164857, 2009.

He, C., Li, Q. B., Liou, K. N., Zhang, J., Qi, L., Mao, Y., Gao, M., Lu, Z., Streets, D. G., Zhang, Q., Sarin, M. M., and Ram, K.: A global 3-D CTM evaluation of black carbon in the Tibetan Plateau, Atmospheric Chemistry and Physics, 14, 7091-7112, doi:10.5194/acp-14-7091-2014, 2014.

Herich, H., Hueglin, C., and Buchmann, B.: A 2.5 year's source apportionment study of black carbon from wood burning and

15   fossil fuel combustion at urban and rural sites in Switzerland, Atmospheric Measurement Techniques, 4, 1409-1420, doi:10.5194/amt-4-1409-2011, 2011.

IPCC: Climate Change 2014: Synthesis Report. Contribution of Working Groups I, II and III to the Fifth Assessment Report of the Intergovernmental Panel on Climate Change, edited by: Core Writing Team, Pachauri, R. K. and Meyer, L. A., IPCC, Geneva, Switzerland, 151 pp, 2014.

20   Jacobson, M. Z.: Short-term effects of controlling fossil-fuel soot, biofuel soot and gases, and methane on climate, Arctic ice, and air pollution health, Journal of Geophysical Research, 115, D14209, doi:10.1029/2009jd013795, 2010.

Jenk, T., Szidat, S., Schwikowski, M., Gäggeler, H., Brütsch, S., Wacker, L., Synal, H.-A., and Saurer, M.: Radiocarbon analysis in an Alpine ice core: record of anthropogenic and biogenic contributions to carbonaceous aerosols in the past (1650–1940), Atmospheric chemistry and physics, 6, 5381-5390, doi: 10.5194/acp-6-5381-2006, 2006.

25   Kodros, J., and Pierce, J.: Important global and regional differences in aerosol cloud‐albedo effect estimates between simulations with and without prognostic aerosol microphysics, Journal of Geophysical Research: Atmospheres, 122, 4003-4018, doi: 10.1002/2016JD025886, 2017.

Konovalov, I. B., Lvova, D. A., Beekmann, M., Jethva, H., Mikhailov, E. F., Paris, J.-D., Belan, B. D., Kozlov, V. S., Ciais, P., and Andreae, M. O.: Estimation of black carbon emissions from Siberian fires using satellite observations of absorption

30   and extinction optical depths, Atmos. Chem. Phys., 18, 14889-14924, https://doi.org/10.5194/acp-18-14889-2018, 2018.

Lee, Y., Chen, K., and Adams, P.: Development of a global model of mineral dust aerosol microphysics, Atmospheric Chemistry and Physics, 9, 2441-2458, doi: 10.5194/acp-9-2441-2009, 2009.

Li, C., Bosch, C., Kang, S., Andersson, A., Chen, P., Zhang, Q., Cong, Z., Chen, B., Qin, D., and Gustafsson, O.: Sources of black carbon to the Himalayan-Tibetan Plateau glaciers, Nat Commun, 7, 12574, doi: 10.1038/ncomms12574, 2016.

Li, M., Zhang, Q., Kurokawa, J.-i., Woo, J.-H., He, K., Lu, Z., Ohara, T., Song, Y., Streets, D. G., Carmichael, G. R., Cheng, Y., Hong, C., Huo, H., Jiang, X., Kang, S., Liu, F., Su, H., and Zheng, B.: MIX: a mosaic Asian anthropogenic emission

5 inventory under the international collaboration framework of the MICS-Asia and HTAP, Atmospheric Chemistry and Physics, 17, 935-963, doi:10.5194/acp-17-935-2017, 2017.

Liu, H., Jacob, D. J., Bey, I., and Yantosca, R. M.: Constraints from 210Pb and 7Be on wet deposition and transport in a global three-dimensional chemical tracer model driven by assimilated meteorological fields, Journal of Geophysical Research: Atmospheres, 106, 12109-12128, doi: 0148-0227/01/2000 JD900839, 2001.

10 Ma, P.-L., Rasch, P. J., Fast, J. D., Easter, R. C., Gustafson Jr, W., Liu, X., Ghan, S. J., and Singh, B.: Assessing the CAM5 physics suite in the WRF-Chem model: Implementation, resolution sensitivity, and a first evaluation for a regional case study, Geoscientific Model Development Discussion, 7, 755, doi:10.5194/gmd-7-755-2014, 2014.

McMeeking, G. R., Morgan, W. T., Flynn, M., Highwood, E. J., Turnbull, K., Haywood, J., and Coe, H.: Black carbon aerosol mixing state, organic aerosols and aerosol optical properties over the United Kingdom, Atmospheric Chemistry and

15 Physics, 11, 9037-9052, doi:10.5194/acp-11-9037-2011, 2011.

Moteki, N., Kondo, Y., Miyazaki, Y., Takegawa, N., Komazaki, Y., Kurata, G., Shirai, T., Blake, D. R., Miyakawa, T., and Koike, M.: Evolution of mixing state of black carbon particles: Aircraft measurements over the western Pacific in March 2004, Geophysical Research Letters, 34, L11803, doi:10.1029/2006gl028943, 2007.

Mouteva, G. O., Randerson, J. T., Fahrni, S. M., Bush, S. E., Ehleringer, J. R., Xu, X., Santos, G. M., Kuprov, R., Schichtel,

20 B. A., and Czimczik, C. I.: Using radiocarbon to constrain black and organic carbon aerosol sources in Salt Lake City, Journal of Geophysical Research: Atmospheres, 122, 9843-9857, doi:10.1002/2017jd026519, 2017.

Park, R. J., Jacob, D. J., Chin, M., and Martin, R. V.: Sources of carbonaceous aerosols over the United States and implications for natural visibility, Journal of Geophysical Research: Atmospheres, 108, 4355, doi: 10.1029/2002jd003190, 2003.

25 Park, R. J., Jacob, D. J., Palmer, P. I., Clarke, A. D., Weber, R. J., Zondlo, M. A., Eisele, F. L., Bandy, A. R., Thornton, D. C., and Sachse, G. W.: Export efficiency of black carbon aerosol in continental outflow: Global implications, Journal of Geophysical Research: Atmospheres, 110, D11205, doi: 10.1029/2004jd005432, 2005.

Petters, M., and Kreidenweis, S.: A single parameter representation of hygroscopic growth and cloud condensation nucleus activity, Atmospheric Chemistry and Physics, 7, 1961-1971, doi: 10.5194/acp-7-1961-2007, 2007.

30 Pierce, J., Chen, K., and Adams, P.: Contribution of primary carbonaceous aerosol to cloud condensation nuclei: processes and uncertainties evaluated with a global aerosol microphysics model, Atmospheric Chemistry and Physics, 7, 5447-5466, doi: 10.5194/acp-7-5447-2007, 2007.

Qi, L., Li, Q., He, C., Wang, X., and Huang, J.: Effects of the Wegener–Bergeron–Findeisen process on global black carbon distribution, Atmospheric Chemistry and Physics, 17, 7459-7479, doi:10.5194/acp-17-7459-2017, 2017a.

Qi, L., Li, Q., Henze, D. K., Tseng, H.-L., and He, C.: Sources of springtime surface black carbon in the Arctic: an adjoint analysis for April 2008, Atmospheric Chemistry and Physics, 17, 9697-9716, doi:10.5194/acp-17-9697-2017, 2017b.

5 Qi, L., Li, Q., Li, Y., and He, C.: Factors controlling black carbon distribution in the Arctic, Atmospheric Chemistry and Physics, 17, 1037-1059, doi:10.5194/acp-17-1037-2017, 2017c.

Reddy, C. M., Pearson, A., Xu, L., McNichol, A. P., Benner, B. A., Wise, S. A., Klouda, G. A., Currie, L. A., and Eglinton, T. I.: Radiocarbon as a tool to apportion the sources of polycyclic aromatic hydrocarbons and black carbon in environmental samples, Environmental Science & Technology, 36, 1774-1782, doi: 10.1021/es011343f , 2002.

10 Sahu, L. K., Kondo, Y., Moteki, N., Takegawa, N., Zhao, Y., Cubison, M. J., Jimenez, J. L., Vay, S., Diskin, G. S., Wisthaler, A., Mikoviny, T., Huey, L. G., Weinheimer, A. J., and Knapp, D. J.: Emission characteristics of black carbon in anthropogenic and biomass burning plumes over California during ARCTAS-CARB 2008, Journal of Geophysical Research: Atmospheres, 117, D16302, doi:10.1029/2011jd017401, 2012.

Samset, B. H., Myhre, G., Schulz, M., Balkanski, Y., Bauer, S., Berntsen, T. K., Bian, H., Bellouin, N., Diehl, T., Easter, R.

15 C., Ghan, S. J., Iversen, T., Kinne, S., Kirkevåg, A., Lamarque, J. F., Lin, G., Liu, X., Penner, J. E., Seland, Ø., Skeie, R. B., Stier, P., Takemura, T., Tsigaridis, K., and Zhang, K.: Black carbon vertical profiles strongly affect its radiative forcing uncertainty, Atmospheric Chemistry and Physics, 13, 2423-2434, doi:10.5194/acp-13-2423-2013, 2013.

Samset, B. H., Myhre, G., Herber, A., Kondo, Y., Li, S. M., Moteki, N., Koike, M., Oshima, N., Schwarz, J. P., Balkanski, Y., Bauer, S. E., Bellouin, N., Berntsen, T. K., Bian, H., Chin, M., Diehl, T., Easter, R. C., Ghan, S. J., Iversen, T., Kirkevåg,

20 A., Lamarque, J. F., Lin, G., Liu, X., Penner, J. E., Schulz, M., Seland, Ø., Skeie, R. B., Stier, P., Takemura, T., Tsigaridis, K., and Zhang, K.: Modelled black carbon radiative forcing and atmospheric lifetime in AeroCom Phase II constrained by aircraft observations, Atmospheric Chemistry and Physics, 14, 12465-12477, doi:10.5194/acp-14-12465-2014, 2014.

Sato, Y., Miura, H., Yashiro, H., Goto, D., Takemura, T., Tomita, H., and Nakajima, T.: Unrealistically pristine air in the Arctic produced by current global scale models, Scientific reports, 6, 26561, doi:10.1038/srep26561, 2016.

25 Schwarz, J. P., Gao, R. S., Spackman, J. R., Watts, L. A., Thomson, D. S., Fahey, D. W., Ryerson, T. B., Peischl, J., Holloway, J. S., Trainer, M., Frost, G. J., Baynard, T., Lack, D. A., de Gouw, J. A., Warneke, C., and Del Negro, L. A.: Measurement of the mixing state, mass, and optical size of individual black carbon particles in urban and biomass burning emissions, Geophysical Research Letters, 35, L13810, doi:10.1029/2008gl033968, 2008.

Shiraiwa, M., Kondo, Y., Moteki, N., Takegawa, N., Miyazaki, Y., and Blake, D. R.: Evolution of mixing state of black

30 carbon in polluted air from Tokyo, Geophysical Research Letters, 34, L16803, doi:10.1029/2007gl029819, 2007.

Subramanian, R., Kok, G., Baumgardner, D., Clarke, A., Shinozuka, Y., Campos, T., Heizer, C., Stephens, B., De Foy, B., and Voss, P. B.: Black carbon over Mexico: the effect of atmospheric transport on mixing state, mass absorption cross-section, and BC/CO ratios, Atmospheric Chemistry & Physics, 10, 219-237, doi:10.5194/acp-10-219-2010, 2010.

Szidat, S., Jenk, T. M., Synal, H.-A., Kalberer, M., Wacker, L., Hajdas, I., Kasper-Giebl, A., and Baltensperger, U.: Contributions of fossil fuel, biomass-burning, and biogenic emissions to carbonaceous aerosols in Zurich as traced by14C, Journal of Geophysical Research, 111, doi:10.1029/2005jd006590, 2006.

Szidat, S., Ruff, M., Perron, N., Wacker, L., Synal, H.-A., Hallquist, M., Shannigrahi, A. S., Yttri, K. E., Dye, C., and Simpson, D.: Fossil and non-fossil sources of organic carbon (OC) and elemental carbon (EC) in Göteborg, Sweden, Atmospheric Chemistry and Physics, 9, 1521-1535, doi: 10.5194/acp-9-1521-2009, 2009.

van der Werf, G. R., Randerson, J. T., Giglio, L., Collatz, G. J., Mu, M., Kasibhatla, P. S., Morton, D. C., DeFries, R. S., Jin, Y., and van Leeuwen, T. T.: Global fire emissions and the contribution of deforestation, savanna, forest, agricultural, and peat fires (1997–2009), Atmospheric Chemistry and Physics, 10, 11707-11735, doi:10.5194/acp-10-11707-2010, 2010.

Wang, Q., Jacob, D. J., Fisher, J. A., Mao, J., Leibensperger, E. M., Carouge, C. C., Le Sager, P., Kondo, Y., Jimenez, J. L., Cubison, M. J., and Doherty, S. J.: Sources of carbonaceous aerosols and deposited black carbon in the Arctic in winter-spring: implications for radiative forcing, Atmospheric Chemistry and Physics, 11, 12453-12473, doi:10.5194/acp-11-12453-2011, 2011.

Winiger, P., Andersson, A., Yttri, K. E., Tunved, P., and Gustafsson, O.: Isotope-Based Source Apportionment of EC Aerosol Particles during Winter High-Pollution Events at the Zeppelin Observatory, Svalbard, Environ Sci Technol, 49, 11959-11966, doi:10.1021/acs.est.5b02644, 2015.

Winiger, P., Andersson, A., Eckhardt, S., Stohl, A., and Gustafsson, Ö.: The sources of atmospheric black carbon at a European gateway to the Arctic, Nature Communications, 7, 12776, doi:10.1038/ncomms12776, 2016.

Winiger, P., Andersson, A., Eckhardt, S., Stohl, A., Semiletov, I. P., Dudarev, O. V., Charkin, A., Shakhova, N., Klimont, Z., Heyes, C., and Gustafsson, O.: Siberian Arctic black carbon sources constrained by model and observation, Proc Natl Acad Sci U S A, 114, E1054-E1061, doi:10.1073/pnas.1613401114, 2017.

Winiger, P., Barrett, T. E., Sheesley, R. J., Huang, L., Sharma, S., Barrie, L. A., Yttri, K. E., Evangeliou, N., Eckhardt, S., Stohl, A., Klimont, Z., Heyes, C., Semiletov, I. P., Dudarev, O. V., Charkin, A., Shakhova, N., Holmstrand, H., Andersson, A., and Gustafsson, Ö.: Source apportionment of circum-Arctic atmospheric black carbon from isotopes and modeling, Science Advances, 5, eaau8052, doi:10.1126/sciadv.aau8052, 2019.

Yamamoto, N., Muramoto, A., Yoshinaga, J., Shibata, K., Endo, M., Endo, O., Hirabayashi, M., Tanabe, K., Goto, S., and Yoneda, M.: Comparison of carbonaceous aerosols in Tokyo before and after implementation of diesel exhaust restrictions, Environmental science & technology, 41, 6357-6362, doi:10.1021/acs.est.5b02644, 2007.

Zhang, Y. L., Perron, N., Ciobanu, V. G., Zotter, P., Minguillón, M. C., Wacker, L., Prévôt, A. S. H., Baltensperger, U., and Szidat, S.: On the isolation of OC and EC and the optimal strategy of radiocarbon-based source apportionment of carbonaceous aerosols, Atmospheric Chemistry and Physics, 12, 10841-10856, doi:10.5194/acp-12-10841-2012, 2012.

Zhang, Y. L., Huang, R. J., El Haddad, I., Ho, K. F., Cao, J. J., Han, Y., Zotter, P., Bozzetti, C., Daellenbach, K. R., Canonaco, F., Slowik, J. G., Salazar, G., Schwikowski, M., Schnelle-Kreis, J., Abbaszade, G., Zimmermann, R., Baltensperger, U., Prévôt, A. S. H., and Szidat, S.: Fossil vs. non-fossil sources of fine carbonaceous aerosols in four

Chinese cities during the extreme winter haze episode of 2013, Atmospheric Chemistry and Physics, 15, 1299-1312, doi:10.5194/acp-15-1299-2015, 2015.

Zotter, P., Ciobanu, V. G., Zhang, Y. L., El-Haddad, I., Macchia, M., Daellenbach, K. R., Salazar, G. A., Huang, R.-J., Wacker, L., Hueglin, C., Piazzalunga, A., Fermo, P., Schwikowski, M., Baltensperger, U., Szidat, S., and Prévôt, A. S. H.: Radiocarbon analysis of elemental and organic carbon in Switzerland during winter-smog episodes from 2008 to 2012 – Part 1: Source apportionment and spatial variability, Atmospheric Chemistry and Physics, 14, 13551- 13570, https://doi.org/10.5194/acp-14-13551-2014, 2014.
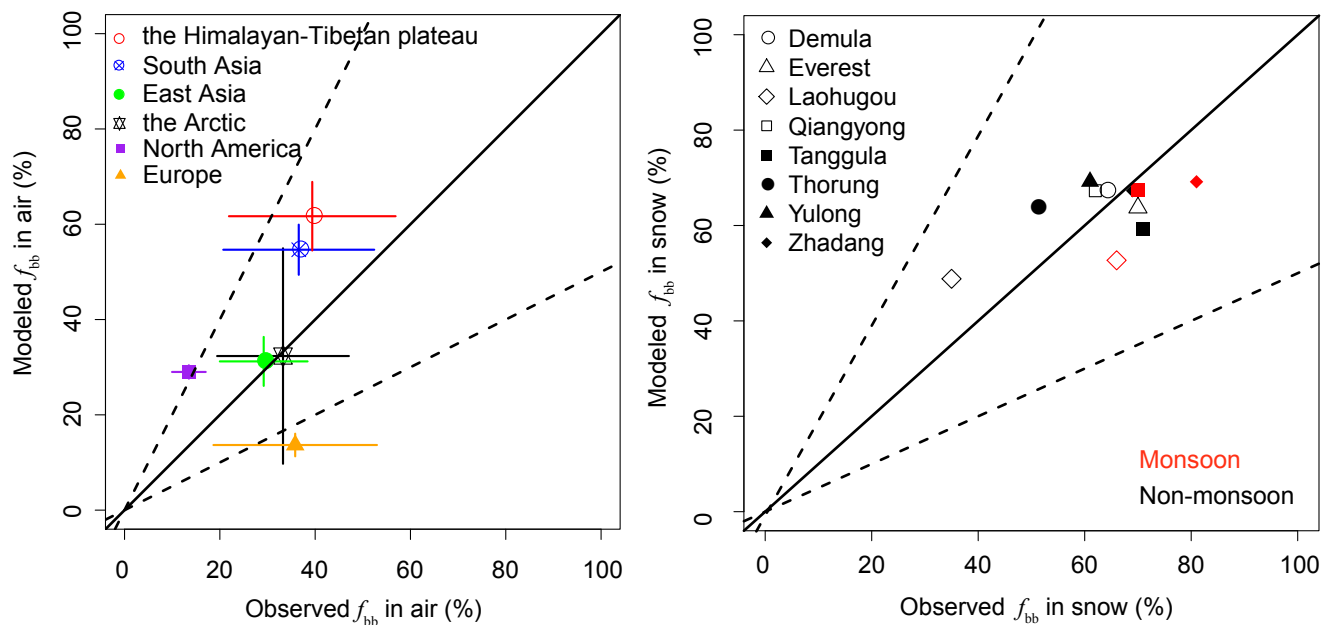
5

Figure 1: Observed and GEOS-Chem simulated fraction of biomass burning (f_{bb}, %) of (a) BC in the atmosphere in the Arctic, South Asia, North America, Europe, East Asia, and the Himalayan-Tibetan plateau (the regions are symbol and color coded, see data in Table S2.) and (b) BC in snow during monsoon (red) and non-monsoon (black) seasons over the Himalayan-Tibetan plateau. Also shown in (a) are the standard deviations of observed and model simulated f_{bb} in each region, reflecting the temporal and spatial variations of f_{bb} in the region (horizontal and vertical lines). Observations of f_{bb} in the atmosphere in (a) are from carbon isotope analysis as listed in Table S1. Observations of f_{bb} in BC in snow in (b) are from Li et al. (2016). Solid lines in (a) and (b) are 1:1 ratio lines and dashed lines are 1:2 (or 2:1).
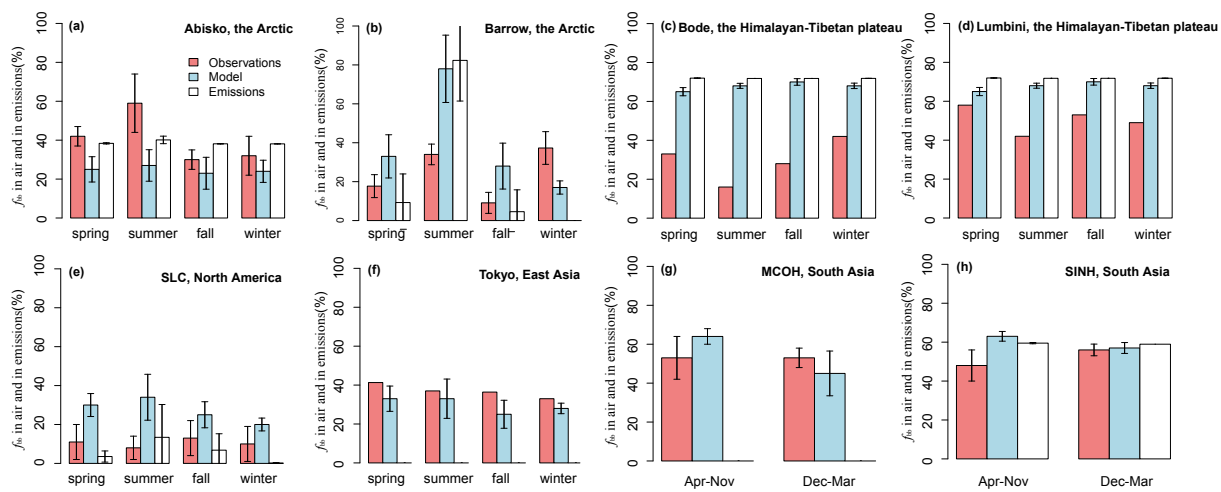
Figure 2: Seasonal variations of observed (lightcoral bars) and GEOS-Chem simulated (lightblue bars) f_{bb} of BC in the atmosphere at (a) Abisko and (b) Barrow in the Arctic, (c) Bode and (d) Lumbini over the Himalayan–Tibetan Plateau, (e) Salt Lake City in North America, (f) Tokyo in East Asia, (g) MCOH and (h) SINH in South Asia. The white bars are f_{bb} values of BC emissions in the model grid (4° lat x 5° lon) of each site. Also shown are the standard deviations (error bars). Site locations are shown in Fig. S3.
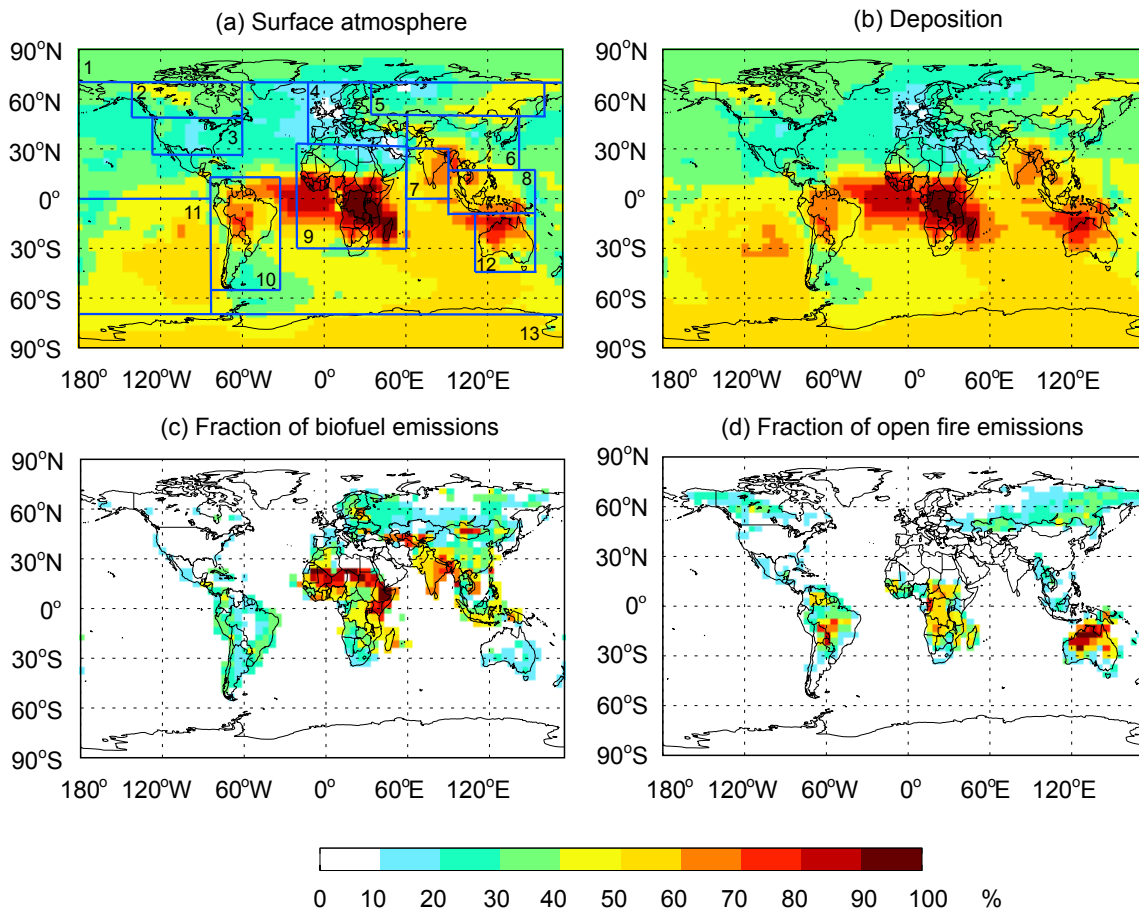
Figure 3: Annual (a) f_{bb} of BC in the atmosphere at surface, (b) f_{bb} of BC deposition, (c) fraction of biofuel emissions and (d) fraction of open fire emissions. Data are averaged for 2007–2013. Also shown in (a) are regions discussed in the text: 1. the Arctic, 2. Canada, 3. the US, 4. Europe, 5. Siberia, 6. East (E.) Asia, 7. South (S.) Asia, 8. Southeast (SE.) Asia, 9. Africa, 10. S. America, 11. S. Pacific, 12. Australia, and 13. the Antarctic.

21
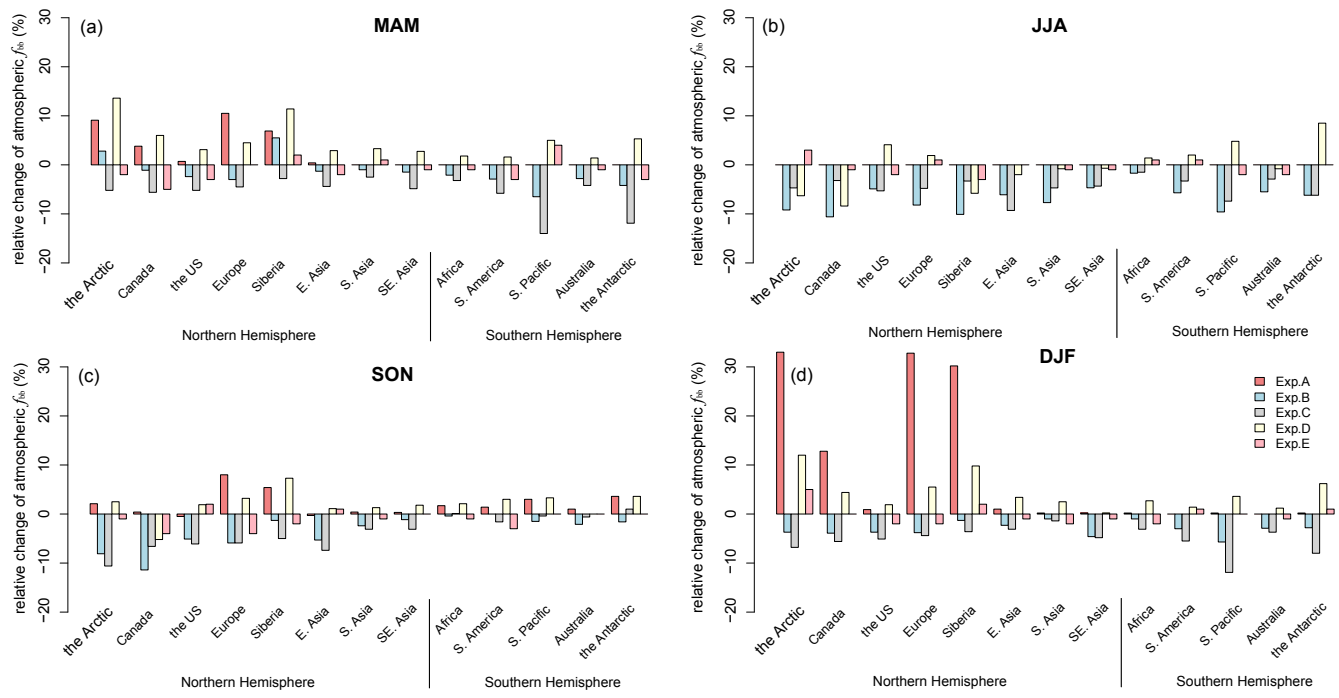
Figure 4: GEOS-Chem simulated fractional change (*r*) to atmospheric f_{bb} relative to the standard simulation, as a result of doubled biofuel emissions north of 45°N (Exp. A), 70% of hydrophilic BC in freshly emitted biomass burning BC-containing particles (Exp. B), 4 hour *e*-folding aging time of BC in biomass burning plumes and linear aging rate of 1% in fossil fuel plumes (Exp. C), TOMAS microphysical aging and scavenging (Exp. D) and finer horizontal model resolution (2° lat × 2.5° lon, Exp. E), $r = ([f_{bb}]_{Exp.} - [f_{bb}]_{Std.})/[f_{bb}]_{Std.}$ that varies with regions (see region definition in Fig.3 (a)) and seasons ((a) March–May (MAM), (b) June–August (JJA), (c) September–November (SON) and (d) December–February (DJF)), averaged for 2007–2013. See details of the standard simulation and the uncertainty experiments in the text.

Table S1. Carbon isotope analysis of BC sources (fossil fuel versus biomass burning) in the atmosphere

Pt	Region	Site	Lat	Lon	Alt (m)	Year	Mon	Season	f_{bb} (%)	BC isolation method	References
1	Arctic	Zeppelin	78.9	11.9	478	2009	Jan-Mar	winter	52±15[5]	NIOSH 5040[6]	Winiger et al., 2015
2	Arctic	Abisko	68.4	19.1	359	2011-13	Jan-Mar	winter	35±10	NIOSH 5040	Winiger et al., 2016
3	Arctic	Abisko	68.4	19.1	359	2011-13	Apr-Aug	summer	58±15	NIOSH 5040	Winiger et al., 2016
4	Arctic	Barrow	71.2	-156.6	11	2012-13	Dec-Feb	winter	32±9	NIOSH 5040	Barrett et al., 2015
5	Arctic	Barrow	71.2	-156.6	11	2012-13	Feb_Mar	winter	51±6	NIOSH 5040	Barrett et al., 2015
6	Arctic	Barrow	71.2	-156.6	11	2013	Mar-May	spring	18±7	NIOSH 5040	Winiger et al., 2019
7	Arctic	Barrow	71.2	-156.6	11	2013	Jul-Aug	summer	34±5	NIOSH 5040	Winiger et al., 2019
8	Arctic	Barrow	71.2	-156.6	11	2013	Sep-Nov	fall	9±5	NIOSH 5040	Winiger et al., 2019
9	Arctic	Barrow	71.2	-156.6	11	2013	Dec-Feb	winter	34±9	NIOSH 5040	Winiger et al., 2019
10	Arctic	Alert	82.3	-62.3	210	2014-15	Feb	winter	39±5	NIOSH 5040	Winiger et al., 2019
12	Arctic	Alert	82.3	-62.3	210	2014-15	Mar	spring	39±5	NIOSH 5040	Winiger et al., 2019
13	Arctic	Alert	82.3	-62.3	210	2014	May	spring	39±5	NIOSH 5040	Winiger et al., 2019
11	Arctic	Alert	82.3	-62.3	210	2014	Jul	summer	37±5	NIOSH 5040	Winiger et al., 2019
14	Arctic	Alert	82.3	-62.3	210	2014	Nov	fall	40±5	NIOSH 5040	Winiger et al., 2019
15	Arctic	Alert	82.3	-62.3	210	2014	Dec	winter	44±5	NIOSH 5040	Winiger et al., 2019
16	Arctic	Tiksi	71.4	128.5	11	2012-14	Mar-May	spring	25±0.2	NIOSH 5040	Winiger et al., 2017
17	Arctic	Tiksi	71.4	128.5	11	2012-14	Jun-Aug	summer	45±0.1	NIOSH 5040	Winiger et al., 2017
18	Arctic	Tiksi	71.4	128.5	11	2012-14	Sep-Nov	fall	48±0.1	NIOSH 5040	Winiger et al., 2017
19	Arctic	Tiksi	71.4	128.5	11	2012-14	Dec-Feb	winter	28±0.2	NIOSH 5040	Winiger et al., 2017
20	South Asia	MCOH[1]	6.8	73.3	15	2006	Jan_Mar	winter	68±6	NIOSH 5040	Gustafsson et al., 2009
21	South Asia	MCOH	6.8	73.3	15	2008-09	Dec_Mar	winter	53±5	NIOSH 5040	Budhavant et al., 2015
22	South Asia	MCOH	6.8	73.3	15	2008-09	Mar_Nov	summer	53±11	NIOSH 5040	Budhavant et al., 2015
23	South Asia	SINH[2]	18.3	73.7	1450	2006	Mar_Apr	spring	46±8	NIOSH 5040	Gustafsson et al., 2009
24	South Asia	SINH	18.3	73.7	1450	2008-09	Dec_Mar	winter	56±3	NIOSH 5040	Budhavant et al., 2015
25	South Asia	SINH	18.3	73.7	1450	2008-09	Mar_Nov	summer	48±8	NIOSH 5040	Budhavant et al., 2015
26	South Asia	Delhi	28.5	77.2	300	2011	Dec-Feb	witner	39	NIOSH 5040	Bikkina et al., 2019
27	South Asia	Delhi	28.5	77.2	300	2011	Mar-May	spring	24	NIOSH 5040	Bikkina et al., 2019
28	South Asia	Delhi	28.5	77.2	300	2011	Jun-Aug	summer	17	NIOSH 5040	Bikkina et al., 2019
29	South Asia	Delhi	28.5	77.2	300	2011	Sep-Nov	fall	31	NIOSH 5040	Bikkina et al., 2019
30	Europe	Göteborg	57.7	11.9	20	2005	Feb	winter	12±4	THEODORE[7]	Szidat et al., 2009
31	Europe	Göteborg	57.7	11.9	20	2006	Jun	summer	12±3	THEODORE	Szidat et al., 2009
32	Europe	Råö	57.3	11.9	10	2005	Feb	winter	38±5	THEODORE	Szidat et al., 2009
33	Europe	Zurich	47.3	8.5	410	2002	Aug	summer	8±1	THEODORE	Szidat et al., 2004
34	Europe	Zurich	47.3	8.5	410	2003	Feb	winter	29±5	THEODORE	Szidat et al., 2006

35	Europe	Zurich	47.3	8.5	410	2003	Mar	spring	15±5	THEODORE	Szidat et al., 2006
36	Europe	Zurich	47.3	8.5	410	2006	Jan	winter	29±4	THEODORE	Sandradewi et al., 2008a
37	Europe	Dübendorf	47.4	8.6	440	2007	Oct	fall	36±3	Swiss_4S[8]	Zhang et al., 2012
38	Europe	Roveredo	46.2	9.1	298	2005	Jan	winter	60±6	THEODORE	Szidat et al., 2007
39	Europe	Roveredo	46.2	9.1	298	2005	Mar	spring	58±6	THEODORE	Szidat et al., 2007
40	Europe	Roveredo	46.2	9.1	298	2005	Dec	winter	74±10	THEODORE	Sandradewi et al., 2008b
41	Europe	Roveredo	46.2	9.1	370	07/08-	Dec-Feb	winter	46	Swiss_4S	Zotter et al., 2014
42	Europe	Moleno	46.3	8.9	254	2005	Feb	winter	17±7	THEODORE	Szidat et al., 2007
43	Europe	Moleno	46.3	8.99	305	07/08-	Dec-Feb	winter	28	Swiss_4S	Zotter et al., 2014
44	Europe	Reiden	47.2	7.9	457	2006	Feb	winter	30±4	THEODORE	Sandradewi et al., 2008a
45	Europe	Reiden	47.2	7.9	510	07/08-	Dec-Feb	winter	34	Swiss_4S	Zotter et al., 2014
46	Europe	Massongex	46.2	6.1	400	2006	Nov	fall	36±4	THEODORE	Perron et al., 2010
47	Europe	Massongex	46.2	6.1	400	2006	Dec	winter	36±4	THEODORE	Perron et al., 2010
48	Europe	Massongex	46.2	6.1	452	08/09-11/12	Dec-Feb	winter	54	Swiss_4S	Zotter et al., 2014
49	Europe	Saxon	46.1	7.1	460	2006	Dec	winter	32±4	THEODORE	Perron et al., 2010
50	Europe	Sion	46.2	7.3	505	2006	Dec	winter	20±3	THEODORE	Perron et al., 2010
51	Europe	Brigerbad	46.3	7.9	650	2006	Dec	winter	31±4	THEODORE	Perron et al., 2010
52	Europe	Payerne	46.8	6.9	456	2006	Jan	winter	60±4	Swiss_4S	Zhang et al., 2012
53	Europe	Payerne	46.8	6.9	456	2006	Jun	summer	44±3	Swiss_4S	Zhang et al., 2012
54	Europe	Payerne	46.8	6.9	539	07/08-11/12	Dec-Feb	winter	51	Swiss_4S	Zotter et al., 2014
55	Europe	Barcelona	41.3	2.1	80	2009	Mar	spring	15±3	adapted THEODORE	Minguillón et al., 2011
56	Europe	Barcelona	41.3	2.1	80	2009	Jul	summer	9±4	adapted THEODORE	Minguillón et al., 2011
57	Europe	Montseny	41.8	2.3	720	2009	Mar	spring	37±4	adapted THEODORE	Minguillón et al., 2011
58	Europe	Montseny	41.8	2.3	720	2009	Jul	summer	23±5	adapted THEODORE	Minguillón et al., 2011
59	Europe	Bern-Bollwerk	46.9	7.6	506	08/09-12/13	Dec-Feb	winter	22	Swiss_4S	Zotter et al., 2014
60	Europe	Sissach-West	47.5	7.8	410	07/08-11/12	Dec-Feb	winter	43	Swiss_4S	Zotter et al., 2014
61	Europe	St.Gallen-Rorschacherstrasse	47.4	9.4	457	07/08-11/12	Dec-Feb	winter	38	Swiss_4S	Zotter et al., 2014
62	Europe	Vaduz-Austrasse	47.1	9.5	706	07/08-11/12	Dec-Feb	winter	45	Swiss_4S	Zotter et al., 2014
63	Europe	Zôrich-Kaserne	47.3	8.5	457	07/08-	Dec-Feb	winter	41	Swiss_4S	Zotter et al., 2014

#	Region	Location	Lat	Lon	Elev	Period	Month	Season	Value	Method	Reference
						11/12					
64	Europe	Basel-St.Johann	47.6	7.6	308	07/08-08/09	Dec-Feb	winter	41	Swiss_4S	Zotter et al., 2014
65	Europe	Solothurn-Altwyberhôsli	47.1	7.6	502	07/08-11/12	Dec-Feb	winter	46	Swiss_4S	Zotter et al., 2014
66	Europe	Sch chental	46.8	8.8	995	10/11-	Dec-Feb	winter	67	Swiss_4S	Zotter et al., 2014
67	Europe	Chiasso	45.8	9	291	07/08-11/12	Dec-Feb	winter	41	Swiss_4S	Zotter et al., 2014
68	Europe	Magadino-Cadenazzo	46.8	6.9	254	07/08-11/12	Dec-Feb	winter	48	Swiss_4S	Zotter et al., 2014
69	Europe	San-Vittore	46.2	9.1	330	07/08-11/12	Dec-Feb	winter	66	Swiss_4S	Zotter et al., 2014
70	North America	Salt Lake City	40.7	-111.8	1426	2012-14	annual	summer	11±1.1	adapted Swiss_4S	Mouteva et al., 2017
71	North America	Mexico City	19.5	-99.1	2240	2006	Mar	spring	16±4	THEODORE	Aiken et al., 2010
72	East Asia	Tokyo	35.6	139.6	40	2004	Oct	fall	36.4	adapted IMPROVE[9]	Yamamoto et al., 2007
73	East Asia	Tokyo	35.6	139.6	40	2004	Dec	winter	33.8	adapted IMPROVE	Yamamoto et al., 2007
74	East Asia	Tokyo	35.6	139.6	40	2004	Feb	winter	32.6	adapted IMPROVE	Yamamoto et al., 2007
75	East Asia	Tokyo	35.6	139.6	40	2004	Apr	spring	41.3	adapted IMPROVE	Yamamoto et al., 2007
76	East Asia	Tokyo	35.6	139.6	40	2004	Jun	summer	37.7	adapted IMPROVE	Yamamoto et al., 2007
77	East Asia	Tokyo	35.6	139.6	40	2004	Aug	summer	35.8	adapted IMPROVE	Yamamoto et al., 2007
79	East Asia	Beijing	39.9	116.4	55	2013	Jan	winter	30±2	Swiss_4S	Zhang et al., 2015
80	East Asia	Beijing	39.9	116.4	55	2013	Jan	winter	26±2	NIOSH 5040	Andersson et al., 2015
81	East Asia	Beijing	39.9	116.4	55	2010	Feb	winter	17±4	NIOSH 5040	Chen et al., 2013
82	East Asia	Shanghai	31.3	121.5	4	2013	Jan	winter	21±2	Swiss_4S	Zhang et al., 2015
83	East Asia	Shanghai	31.3	121.5	4	2013	Jan	winter	32±2	NIOSH 5040	Andersson et al., 2015
84	East Asia	Shanghai	31.3	121.5	4	2010	Jan	winter	17±4	NIOSH 5040	Chen et al., 2013
85	East Asia	Guangzhou	23.1	113.4	15	2013	Jan	winter	48±5	Swiss_4S	Zhang et al., 2015
86	East Asia	Guangzhou	23.1	113.4	15	2013	Jan	winter	32±2	NIOSH 5040	Andersson et al., 2015
89	East Asia	Xi'an	34.2	108.9	416	2013	Jan	winter	25±3		Zhang et al., 2015
90	East Asia	Xiamen	24.5	118	2	2009	Dec	winter	13±3	NIOSH 5040	Chen et al., 2013
93	East Asia	KCOG[3]	33.3	126.2	72	2011	Mar	winter	25±6	NIOSH 5040	Chen et al., 2013
94	East Asia	SCCO[4]	24.6	118.1	3	2009	Jan	winter	22±3	NIOSH 5040	Chen et al., 2013
95	Tibet	Jilong	28.2	86	4166	2013	Apr	spring	45	NIOSH 5040	Li et al., 2016
96	Tibet	Jilong	28.2	86	4166	2013	Jun	winter	41	NIOSH 5040	Li et al., 2016
97	Tibet	Nielamu	28.2	86	4166	2013	Nov	fall	40	NIOSH 5040	Li et al., 2016
98	Tibet	Dhunche	28.1	85.3	2051	2014	Jan	winter	49	NIOSH 5040	Li et al., 2016
99	Tibet	Dhunche	28.1	85.3	2051	2013	Aug	summer	16	NIOSH 5040	Li et al., 2016

100	Tibet	Dhunche	28.1	85.3	2051	2013	Sep	fall	41	NIOSH 5040	Li et al., 2016
101	Tibet	Bode	27.7	85.4	1386	2014	Jan	winter	42	NIOSH 5040	Li et al., 2016
102	Tibet	Bode	27.7	85.4	1386	2013	Apr	spring	33	NIOSH 5040	Li et al., 2016
103	Tibet	Bode	27.7	85.4	1386	2013	Aug	summer	16	NIOSH 5040	Li et al., 2016
104	Tibet	Bode	27.7	85.4	1386	2013	Nov	fall	28	NIOSH 5040	Li et al., 2016
105	Tibet	Zhongba	29.7	84	4704	2013	Apr	spring	70	NIOSH 5040	Li et al., 2016
106	Tibet	Jomsom	28.8	83.7	3048	2013	Apr	spring	57	NIOSH 5040	Li et al., 2016
107	Tibet	Pokhara	28.2	84	813	2013	Jul	summer	26	NIOSH 5040	Li et al., 2016
108	Tibet	Pokhara	28.2	84	813	2013	Apr	spring	65	NIOSH 5040	Li et al., 2016
109	Tibet	Lumbini	27.5	83.3	100	2013	Apr	spring	58	NIOSH 5040	Li et al., 2016
110	Tibet	Lumbini	27.5	83.3	100	2013	Jul	summer	42	NIOSH 5040	Li et al., 2016
111	Tibet	Lumbini	27.5	83.3	100	2013	Oct	fall	53	NIOSH 5040	Li et al., 2016
112	Tibet	Lumbini	27.5	83.3	100	2013	Dec	winter	49	NIOSH 5040	Li et al., 2016
113	Tibet	Namco	30.8	91	4730	2013	Apr	spring	54	NIOSH 5040	Li et al., 2016
114	Tibet	Namco	30.8	91	4730	2014	Jun	summer	63	NIOSH 5040	Li et al., 2016
115	Tibet	Namco	30.8	91	4730	2014	Jul	summer	49	NIOSH 5040	Li et al., 2016
116	Tibet	Namco	30.8	91	4730	2013	Nov	fall	58	NIOSH 5040	Li et al., 2016
117	Tibet	Lulang	29.8	94.7	3326	2014	Jun	summer	20	NIOSH 5040	Li et al., 2016
118	Tibet	Lulang	29.8	94.7	3326	2014	Jul	summer	23	NIOSH 5040	Li et al., 2016
119	Tibet	Lhasa	29.6	91	3640	2014	Jan	winter	18	NIOSH 5040	Li et al., 2016
120	Tibet	Lhasa	29.6	91	3640	2013	Apr	spring	24	NIOSH 5040	Li et al., 2016
121	Tibet	Lhasa	29.6	91	3640	2013	Jun	summer	7	NIOSH 5040	Li et al., 2016

[1] Maldives Climate Observatory in Hanimaadhoo

[2] Indian Institute of Tropical Meteorology in Sinhagad, India

[3] Korea Climate Observatory-Gosan

[4] South China Climate Observatory

[5] Standard deviation of observations

[6] National Institute for Occupational Safety and Health 5040

[7] Two-step Heating system for the EC/OC Determination of Radiocarbon in the Environment

[8] four-step (S1, S2, S3 and S4) thermal-optical protocol

[9] Integragency Monitoring of Protected Visual Environments

Table S2 Observed and GEOS-Chem simulated atmospheric f_{bb} in various regions (%)

| Region	Observations	Simulation
The Himalayan-Tibetan plateau	39±17*	62±7
South Asia	37±16	55±5
East Asia	29±9	31±5
The Arctic	33±14	32±23
North America	14±4	29±2
Europe	43±16	14±3

*Standard deviation, reflecting variations of atmospheric f_{bb} among different sites during different seasons in each region.
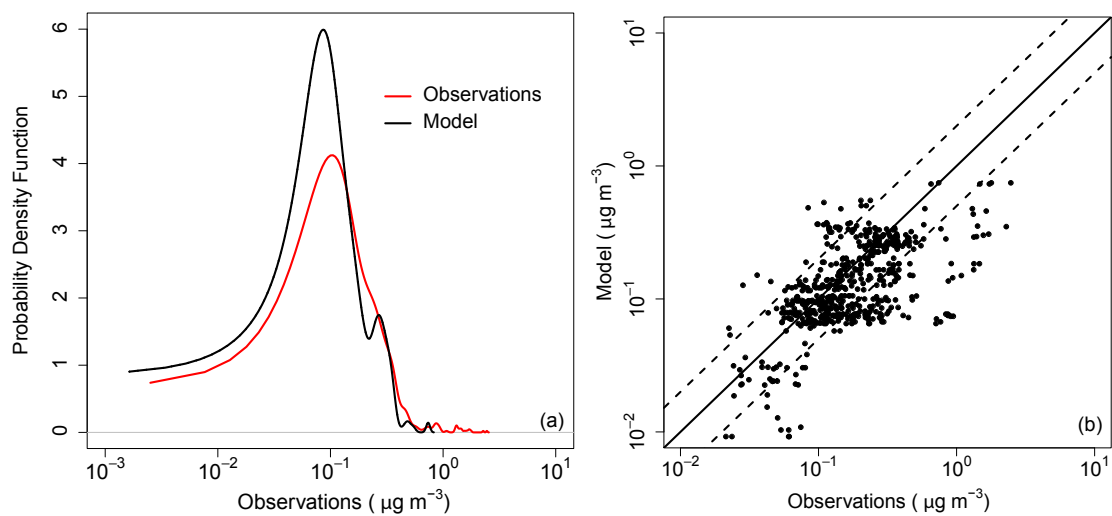
Figure S1. (a) Probability density function of observed (red line) and GEOS-Chem simulated (black) BC concentrations in surface air (µg m^{-3}) and (b) Observed and GEOS-Chem simulated annual BC concentrations in surface air. Data are for 2007–2013. Solid line is 1:1 ratio line and dashed lines are 1:2 (or 2:1).
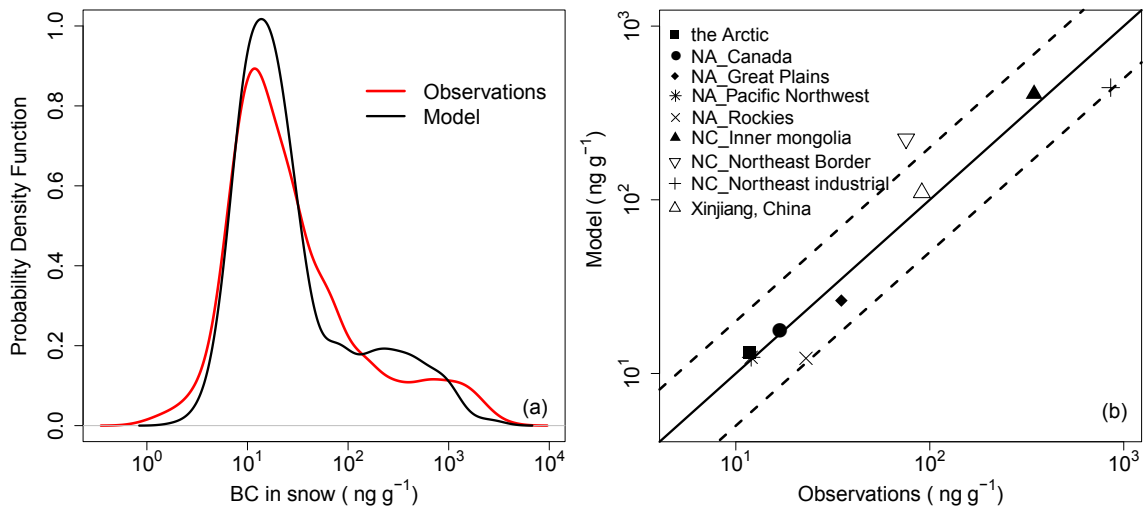
Figure S2. (a) Probability density function of observed (red line) and GEOS-Chem simulated (black) BC concentration in snow (ng g^{-1}) and (b) medians of observed and simulated BC in snow (ng g^{-1}) in the Arctic, North America (Canada, the Great Plains, the Pacific Northwest, and the Rockies, as defined in Doherty et al., 2014)), Northern China (Inner Mongolia, Northeast Border and Northeast Industrial, as defined by Wang et al., 2013), and Xinjiang, China. The regions are symbol-coded. Solid line – 1:1 ratio line; dashed lines – 1:2 (or 2:1) ratio lines.
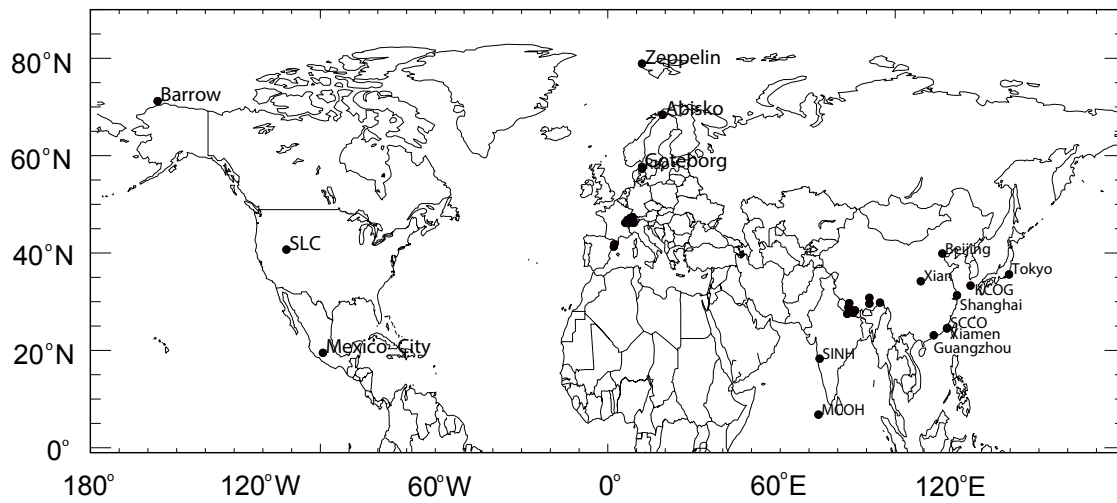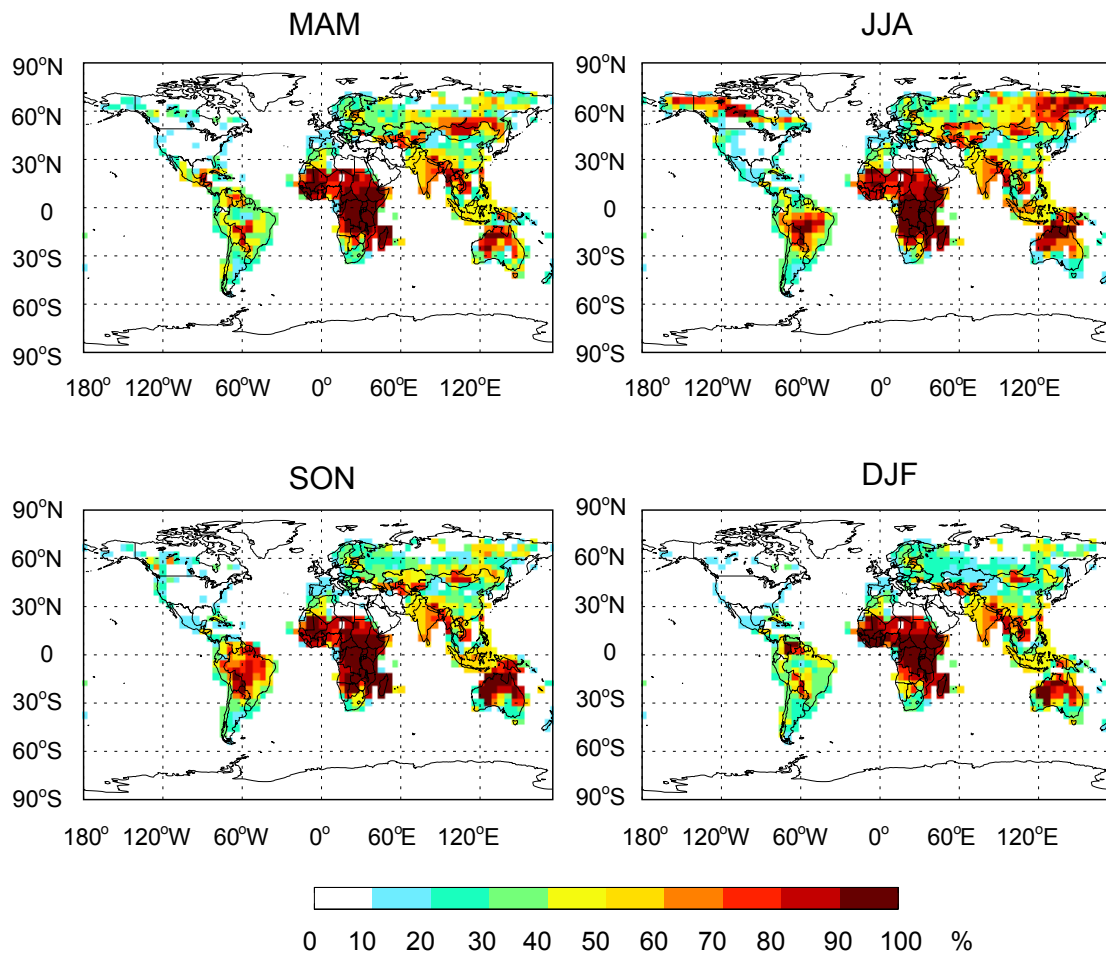
Figure S3. Carbon isotope measurement stations of BC as listed in Table S1.
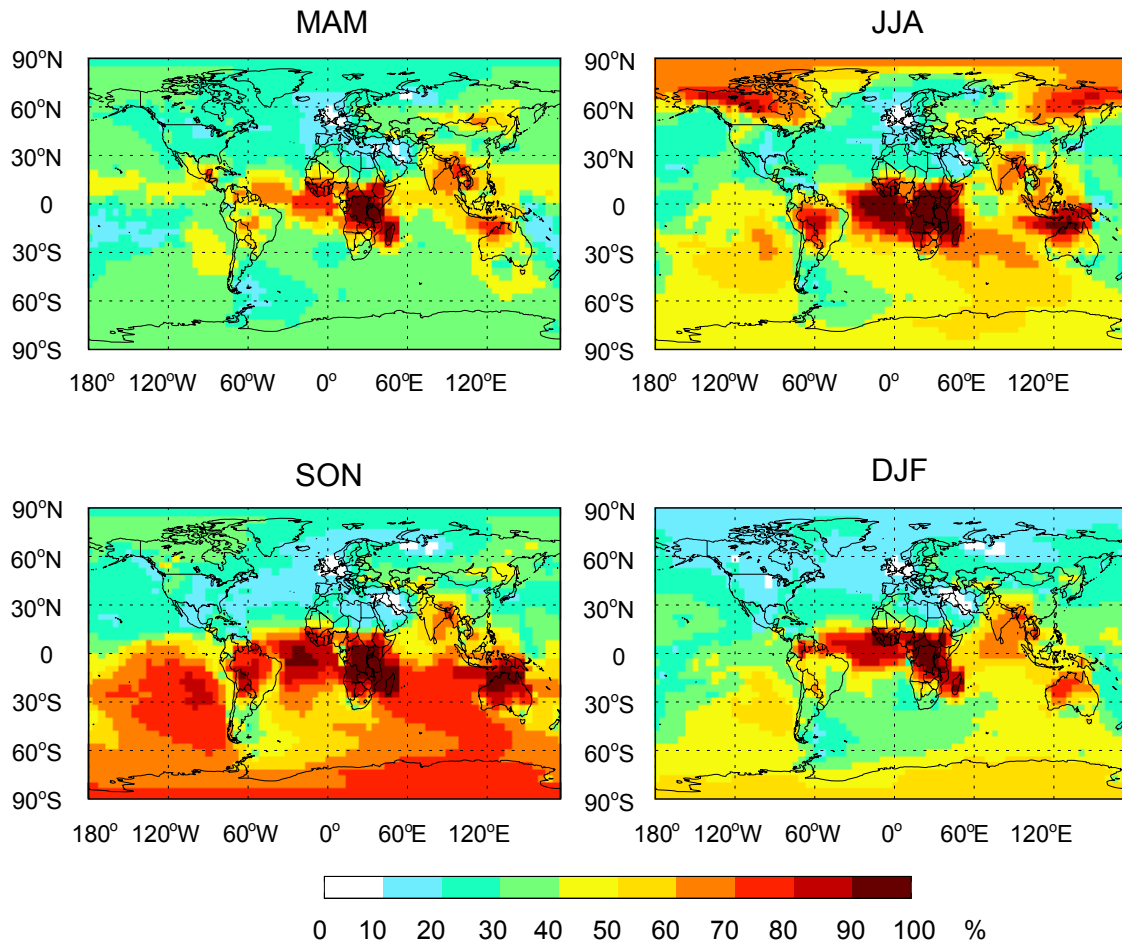
Figure S4. Average f_{bb} of BC in surface atmosphere during March–May (MAM), June–August (JJA), September–November (SON) and December–February (DJF) for 2007–2013.
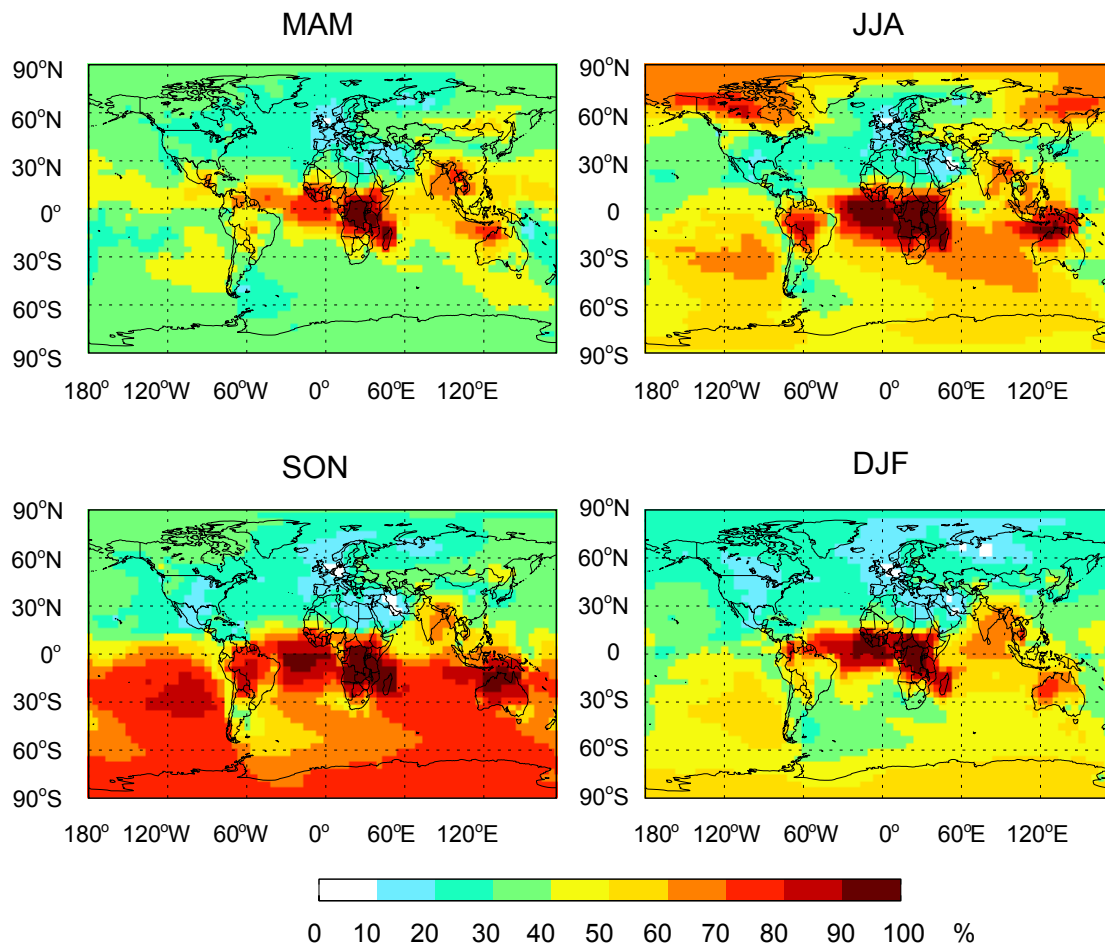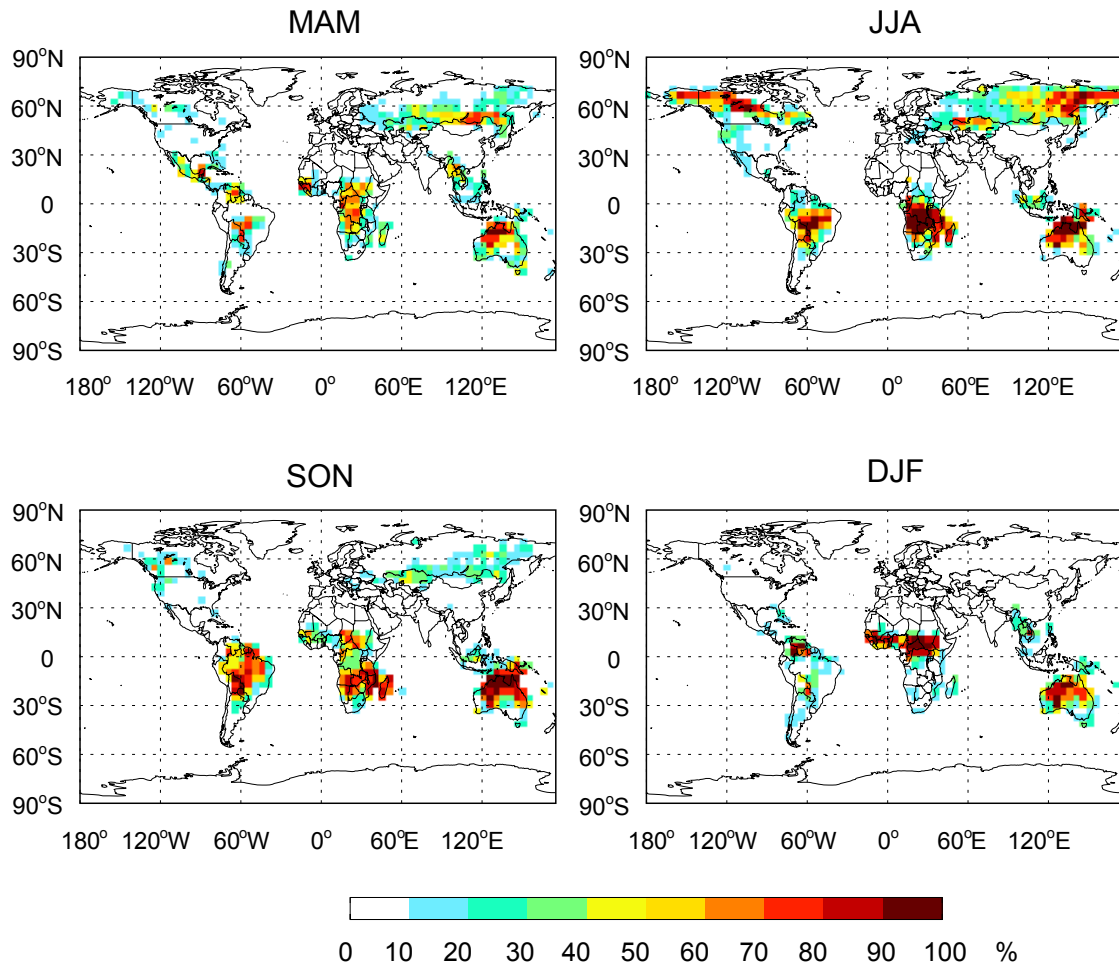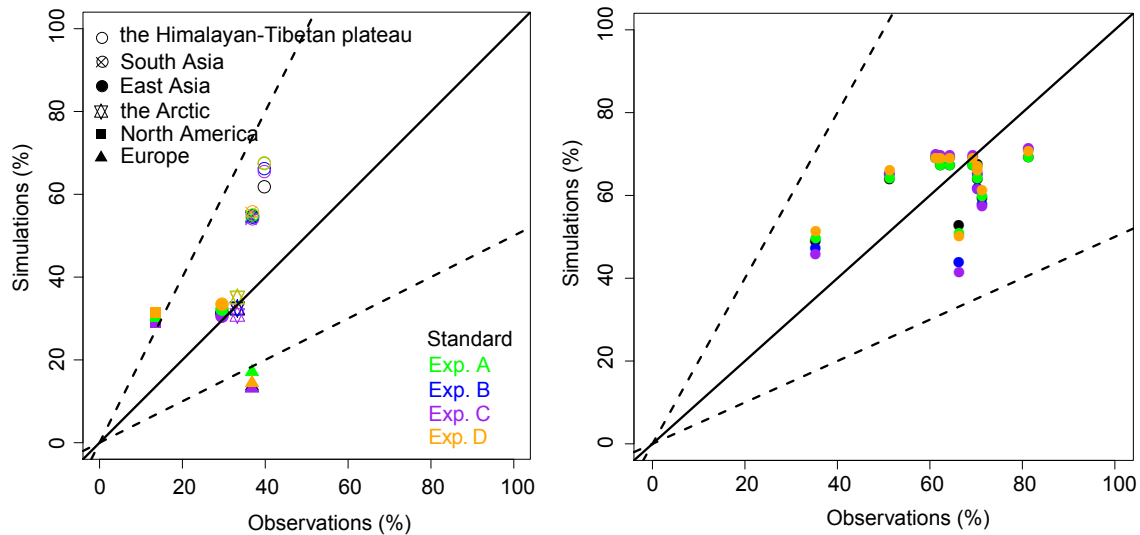
Figure S5. Same as Figure S4, but for BC deposition.

Figure S6. Same as Figure S4, but for BC emissions.

Figure S7. Average contribution of open burning to BC emissions (%) during March–May (MAM), June–August (JJA), September–November (SON) and December–February (DJF) for 2007–2013.

Figure S8. Observed and GEOS-Chem simulated mean f_{bb} (%) (a) of BC in the atmosphere in the six regions in Northern Hemisphere and (b) of BC deposited in snow over the Tibetan plateau. The regions are symbol-coded and the simulations are color-coded (see text for details). Solid lines are 1:1 and dashed lines are 1:2 (or 2:1).